**Newsletters on Stratigraphy, Vol. 50/3 (2017), 245–267** **Article**
Published online February 2017; published in print June 2017

# Changes to sea-surface characteristics during the middle Eocene (47.4 Ma) C21r-H6 event: evidence from calcareous nannofossil assemblages of the Gorrondatxe section (western Pyrenees)

**Beñat Intxauspe-Zubiaurre[1]*, Aitor Payros[1], José-Abel Flores[2], and Estibaliz Apellaniz[1]**

With 5 figures, 1 plate and 2 appendices

**Abstract.** The study of Eocene hyperthermal events is crucial to deciphering the potential responses of the environment to different global warming scenarios. To this end, the present study characterizes the calcareous nannofossil assemblages from the C21r-H6 (47.48 to 47.22 Ma) event of the Gorrondatxe section, thus providing new insights into the environmental impact of this carbon-cycle perturbation event on ocean surface waters. The proportion of reworked calcareous nannofossils was found to increase notably during the event, representing up to 40 % of the assemblage, whereas the number of autochthonous calcareous nannofossils decreased due to dilution with terrigenous material. Autochthonous taxa were found not to show significant changes, as only the abundance of warm and oligotrophic indicators decreased slightly. Hardy taxa that inhabited epicontinental environments and were able to adapt to drastic changes in shallow water characteristics, such as salinity, peaked within the core of the event. This scenario strongly suggests that temperature was not the main factor controlling the distribution of calcareous nannofossil assemblages in the Gorrondatxe area during the core of the C21r-H6 event. The combination of a coeval decrease in $\delta^{13}C$ and an increase in clay minerals (especially kaolinite) suggests increased continental input to the ocean. Therefore, it can be assumed that terrestrial input increased as a consequence of intensified hydrologic cycle and weathering on land, also suggesting increased freshwater input into the oceans. This interpretation supports the hypothesis that increased silicate weathering leads to a reduction in atmospheric $CO_2$ levels.

**Key words.** Hyperthermal, calcareous nannofossils, continental input, reworking, Eocene

## 1. Introduction

The early – middle Eocene times were characterized by warm temperatures punctuated by several short-lived (tens to hundreds of kyr) extreme warming events, commonly referred to as hyperthermals (Thomas and Zachos 2000, Zachos et al. 2001). In addition to low $\delta^{18}O$ values, the hallmarks of these hyperthermal

**Authors' addresses:**
[1] Department of Stratigraphy-Paleontology, Faculty of Science and Technology, University of the Basque Country (UPV/EHU), P.O. Box 644, E-48080 Bilbao, Spain. benat.intxauspe@ehu.eus, a.payros@ehu.eus, estibaliz.apellaniz@ehu.eus
[2] Departamento de Geología, Facultad de Ciencias, Universidad de Salamanca. Plaza de los Caídos s/n, 37008 Salamanca, Spain. flores@usal.es.
* Corresponding author: benat.intxauspe@ehu.eus


DOI: 10.1127/nos/2017/0305
www.borntraeger-cramer.de
0078-0421/2017/0305 $ 5.75

events include negative excursions in the $\delta^{13}C$ record, suggesting that $^{13}C$-depleted carbon was released into the ocean-atmosphere system (Dickens et al. 1995, Zachos et al. 2004, 2008). The hyperthermal events caused severe environmental perturbations, such as increased rainfall and runoff on land, shallowing of the calcium carbonate compensation depth (CCD), and transient biological changes (Kennett and Stott 1991, Bice and Marotzke 2000, Schmitz et al. 2000, Nicolo et al. 2007, Stap et al. 2009). The recovery from these events was commonly driven by increased silicate weathering on land, which reduced the concentration of atmospheric $CO_2$ and caused seawater alkalinization (Jiang and Wise 2006, Agnini et al. 2009, Krishnan et al. 2014, Penman 2016).

Consequently, the Eocene hyperthermal events can be used as reference models to improve our understanding of ongoing climate change (Masson-Delmotte and Schulz, 2013). The most prominent hyperthermal event, the Paleocene–Eocene Thermal maximum (PETM) has been thoroughly studied using calcareous nannofossils (Agnini et al. 2007, Giusberti et al. 2007, Raffi and De Bernardi 2009, Gibbs et al. 2010). Conversely, much less attention has been paid to shorter hyperthermal events, such as the Eocene Thermal Maximum (ETM) 2 and ETM3, despite the fact that their characterization is crucial to deciphering the potentially variable responses of calcareous phytoplankton to different global warming scenarios (Cramer et al. 2003, Röhl et al. 2005, Lourens et al. 2005, Villa et al. 2008, Kirtland-Turner et al. 2014).

The aim of this study is therefore to redress the balance by analyzing one of the minor Eocene hyperthermal events, namely the Lutetian C21r-H6 event exposed at the Gorrondatxe section (Sexton et al. 2011, Payros et al. 2012). While previous studies carried out in Gorrondatxe have focused on physical and geochemical aspects combined with benthic foraminifera and ichnological data from seabed deposits (Payros et al. 2012), the present study aims to decipher the impact of the C21r-H6 event on calcareous nannoplankton (Coccolithophores) assemblages. In today's oceans, the abundance of Coccolithophores is largely dependent on factors such as temperature, nutrients, water stratification and pH (Wei and Wise 1990, Aubry 1992, 1998, Bralower 2002). Consequently, the environmental preferences of some calcareous nannofossil groups can be used to interpret Eocene environmental changes, including some on hyperthermal events (Monechi et al. 2000, Orue-Etxebarria et al. 2004, Tremolada and Bralower 2004, Raffi et al. 2009, Schneider et al. 2011).

## 2. Geological setting

The studied succession is exposed at the cliff of the Gorrondatxe beach (south-eastern coast of the Bay of Biscay, Lat. 43° 23′ N Long. 3° 01′ W; Fig. 1), which hosts the Global Stratotype Section and Point for the base of the Lutetian Stage (Molina et al. 2011). This section is part of a 2300-m-thick deep-marine sedimentary succession, which accumulated on a rapidly subsiding basin during early–middle Eocene times (Payros et al. 2006). Located at the bottom of a 1500 m deep gulf that opened into the Atlantic Ocean at 35° N paleolatitude (Smith 1996), the area was part of the North Iberian continental margin. Despite the location, however, according to Eocene climate and ocean circulation reconstructions (Bice and Marotzke 2000, Huber and Sloan 2000), Gorrondatxe was not in an upwelling area.

The lower Lutetian succession is composed of alternating pelagic limestones and marls interspersed with thin-bedded turbidites, which form recurrent tripartite sequences, generally 10–40 cm thick, consisting of a basal thin-bedded sandy turbidite (with divisions Ta to Td of the Bouma sequence), its capping grey clay (division Te of the Bouma sequence) and a whitish pelagic mudstone (Payros et al. 2007, 2009, Payros and Martínez-Braceras 2014). In addition, Payros et al. (2012) identified an anomalous interval (118–148 m in Fig. 2) characterized by a distinctively low carbonate content and increased abundance of turbidites and kaolinite. This interval is also typified by a $> 1‰$ decline in benthic foraminiferal $\delta^{13}C$ followed by a gradual recovery, a distinct deterioration in foraminiferal preservation, high proportions of warm-water planktic foraminifera and opportunistic benthic foraminifera, and reduced trace fossil and benthic foraminifera diversity. Payros et al. (2012) interpreted that these anomalous charactertistics recorded a significant paleoenvironmental perturbation, which occurred within calcareous nannofossil Zone NP14 and lasted 226 kyr (47.44–47.214 Ma). Taking everything into account, they divided the Gorrondatxe section into four distinct intervals (Fig. 2): A) pre-event succession (0–118 m); B) core of the event (118–133 m), which records peak anomaly conditions; C) initial recovery (133–148 m); and D) aftermath of the event (148–200 m), which began with a transient overcompensation phase in which the pre-perturbation carbonate content and $\delta^{13}C$ values were temporarily exceeded (148–158 m) but subsequently returned to normal environmental conditions.

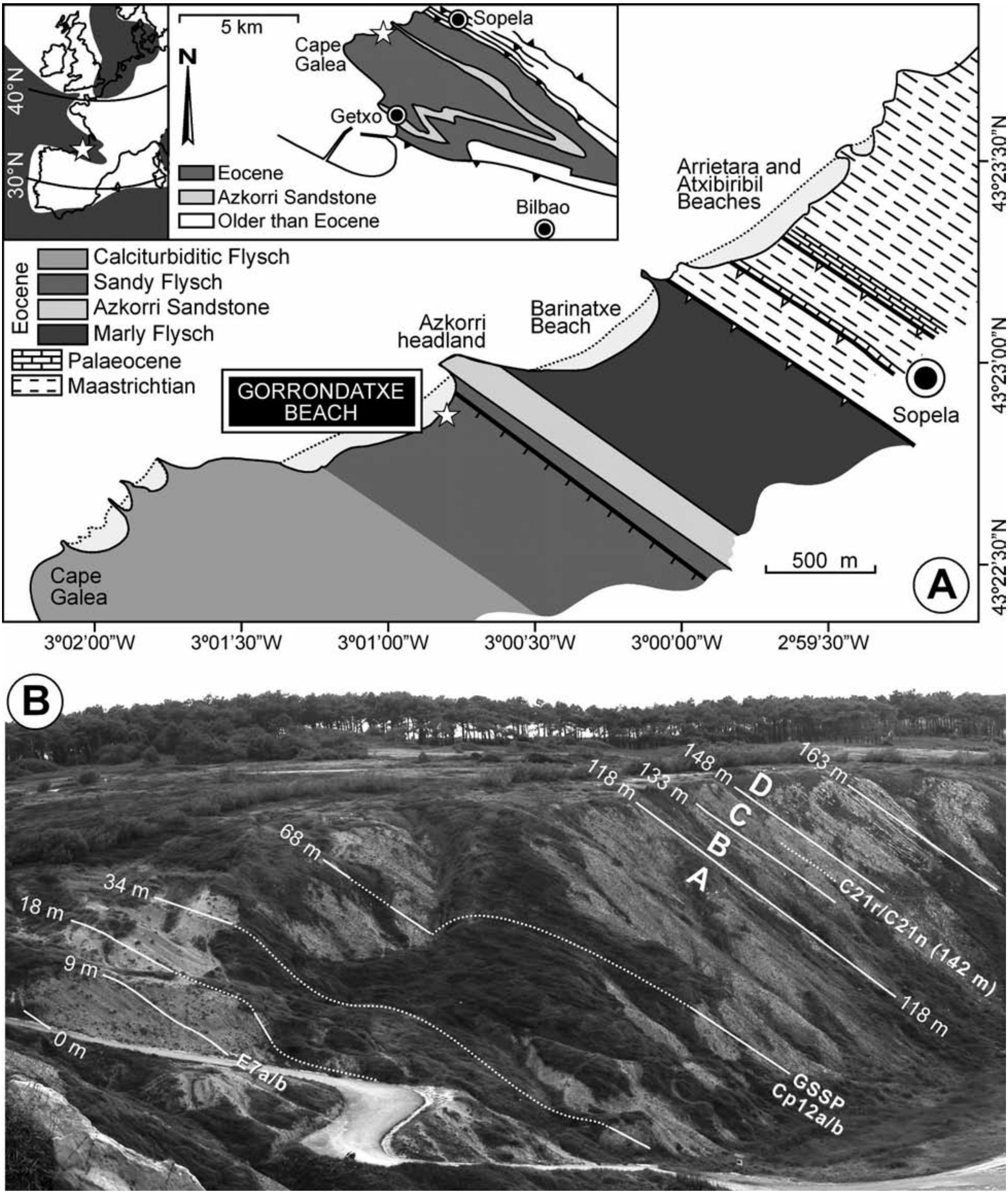


**Fig. 1.** (A) Simplified paleogeographic and geological maps of the Gorrondatxe area, showing (paleo)location of the studied section (star). (B) General view of the Gorrondatxe section, showing reference levels and the extension of the C21r-H6 event (intervals B, C and lowermost part of D).

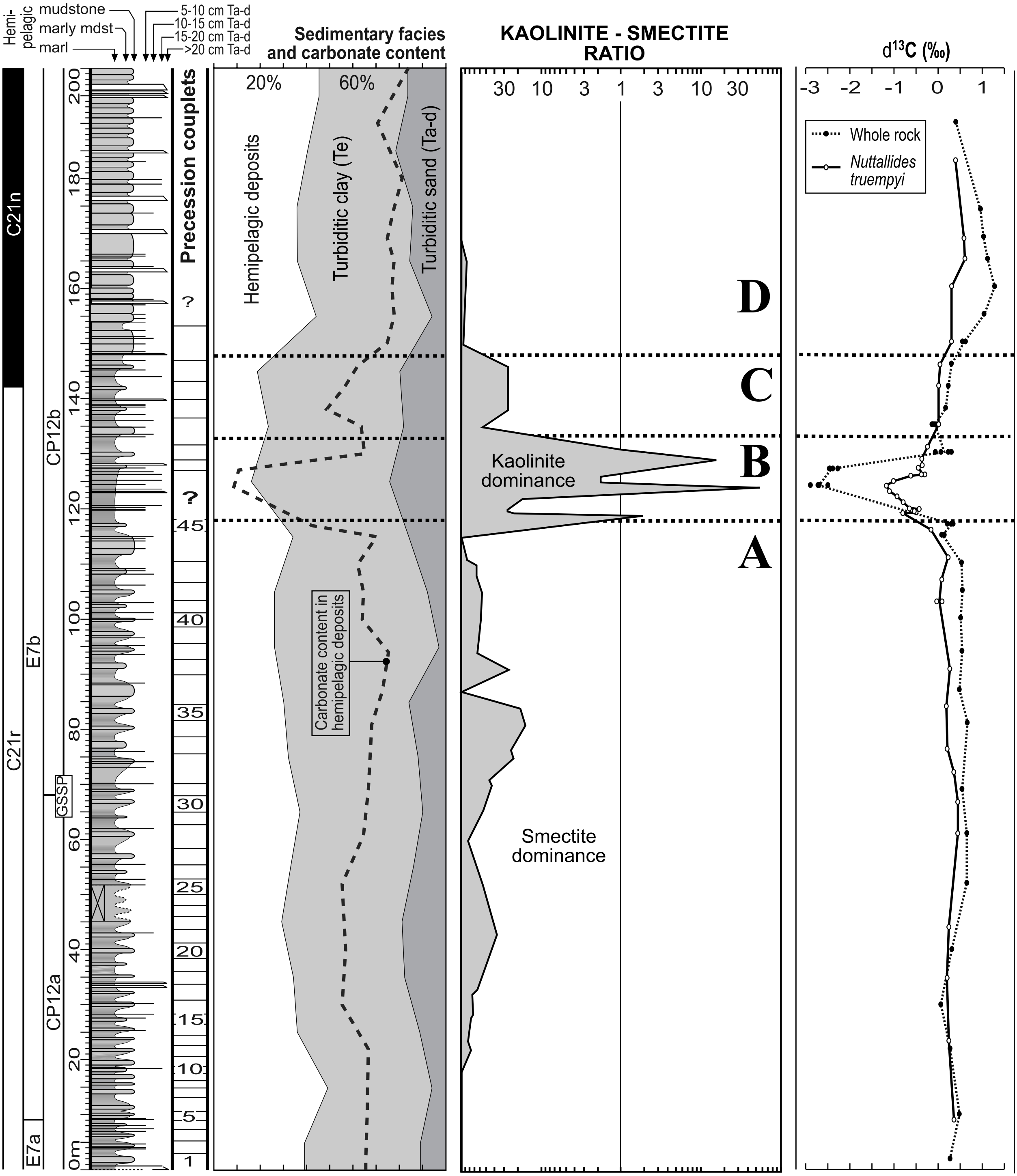


**Fig. 2.** Lithological log of the Gorrondatxe section (compiled from Payros et al. 2012), showing chronostratigraphy, precession-driven mudstone-marl couplets, variations in the percentage of turbiditic and hemipelagic sediments, and their carbonate content. The kaolinite/smectite clay mineral ratio is plotted on a two-sided, symmetric semilogarithmic graph as the percentage of deviation from an assumed content in each mineral of 50 %. Stable isotope ($\delta^{13}C$) results were obtained from both hemipelagic mudstones (whole rock) and from the benthic foraminifer *Nuttallides truempyi*. A, B, C and D correspond to the stratigraphic intervals defined by Payros et al. (2012), which were attributed to pre-C21r-H6 deposits, core of the C21r-H6 event, subsequent recovery, and aftermath of the event, respectively. The succession studied herein extends from 98 to 180 m.

Payros et al. (2012) correlated these short-term changes with the C21r-H6 event (Sexton et al. 2011), which was originally described as a hyperthermal event produced by a perturbation in the global carbon-cycle. The latter authors showed that in the tropical western Atlantic Ocean (ODP Site 1258) the C21r-H6 event is characterized by a 0.7‰ decrease in $\delta^{13}C$ and a 0.4‰ decrease in benthic foraminifera $\delta^{18}O$, suggesting a 2 °C warming of bottom waters. These stable isotope changes correlate with increased carbonate dissolution at 2000–3000 m paleodepth in the South Atlantic and Pacific oceans, pointing to a global increase in deep ocean acidity and a rise of the lysocline (Sexton et al. 2011). Payros et al. (2012) added that a coeval carbonate-barren interval also occurs in the western North Atlantic Ocean (ODP Site 647, Labrador Sea; Firth et al. 2012).

## 3. Materials and methods

An 82 m thick section of the Gorrondatxe succession, which corresponds to the interval from 98 to 180 m in Figure 2, was sampled to study calcareous nannofossils. In order to obtain a complete record throughout the C21r-H6 event, the sampling included the uppermost 20 m of pre-event Interval A (98–118 m), Interval B (118–133 m), Interval C (133–148 m), the aftermath of the event in Interval D (148–158 m), and 24 m of the overlying succession (158–182 m). One hundred and twenty-eight samples were collected, but sampling resolution varied along the section. Thus, in most of Interval A (98–114 m) samples were collected every 80 cm. The spacing was reduced to 30 cm in the uppermost 4 m of Interval A and throughout Interval B (114–133 m). Sample spacing increased again to 80 cm in Interval C and the lowermost 14 m of Interval D (133–162 m). In the rest of the succession (162–182 m), spacing increased progressively from 1.4 m to 2 m.

Given that pelagic mudstones were too hard for the extraction of microfossils, all samples were collected at the transition from turbiditic grey marls to overlying whitish pelagic mudstones, where primary mixing and the addition of allochthonous specimens by turbidity currents are assumed to be minimal. The samples were dried in an oven and subsequently 4 mg were extracted and distributed homogeneously on a coverslip using the decantation method proposed by Flores and Sierro (1997). The coverslips were then glued to smear slides using Canada balsam.

Smear slides were analyzed under a Leica DMLP transmitted light microscope at 1250X magnification. In this study, calcareous nannofossils include all heterococcoliths, holococcoliths and nannoliths incertae sedis. Several information sources were used for the classification of the calcareous nannofossil taxa (Plate 1). The taxonomy mainly follows the concepts in the reference work "Cenozoic calcareous nannofossils" (Perch-Nielsen, 1985) and in the updated online dataset Nannotax (http://ina.tmsoc.org/Nannotax3/index.php?dir=Coccolithophores). A list of all the taxa identified in Gorrondatxe, alongside their stratigraphic ranges and relevant references, is available in Appendix 1.

Mesozoic and Paleocene taxa were readily classified as reworked specimens. Recognition of some Eocene reworked taxa was also straightforward, as they were extinct by Zone NP14 times (e.g., *Calciosolenia*, *Craticulithus*, *Ellipsolithus*, *Fasciculithus*, *Heliolithus*, *Hornibrookina*, *Neochiastozygus*, *Prinsius* and *Toweius*). However, the first appearances of some taxa which characterize Zone NP14 occurred earlier in the stratigraphic record, meaning that it was not possible to determine if they were autochthonous or reworked. For the purposes of this study, it was assumed that all NP14 taxa were autochthonous.

In order to characterize the calcareous nannofossil assemblages and detect rare species with biostratigraphic or paleoecological significance, around 500 specimens (autochthonous and reworked) were counted and classified on each smear slide. According to Denisson and Hay (1967), this procedure guarantees the recognition of every taxon exceeding 1 % of the total assemblage. The reworked/autochthonous proportion was calculated by dividing the number of reworked specimens by the total number (autochthonous and reworked) of calcareous nannofossils (Fig. 3).

Subsequently, the number of autochthonous specimens per $mm^2$ was calculated following the method below (Fig. 3). First, the average number of autochthonous specimens on each field of view was counted and then, based on the area of the field of view and assuming that the sample had been homogeneously distributed, the figure was expressed as specimens per $mm^2$. Additionally, in order to check whether dissolution affected the composition of calcareous nannofossil assemblages, the distribution of taxa susceptible to dissolution, such as *Reticulofenestra minuta* and *Zygrhablithus bijugatus*, was analyzed (Adelseck 1973, Bralower 2002, Jiang and Wise 2006, Raffi et al. 2009).

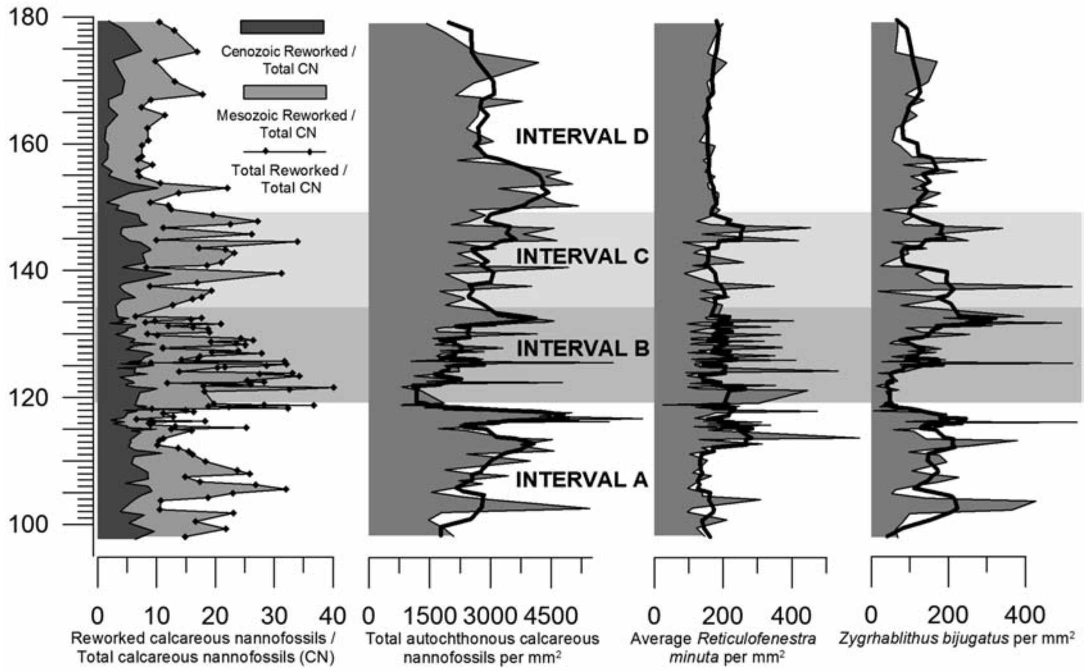


**Fig. 3.** Calcareous nannofossil assemblage variations found throughout the studied section, including the stratigraphic distribution of reworked taxa in proportion to the whole assemblage, the number of autochthonous calcareous nannofossils per mm$^2$ and relative abundances of environmentally significant autochthonous taxa (see Appendix 2 for quantitative data). The thick black curves show 5-point running mean values and illustrate general trends. Note that scale-bars are different for each case.

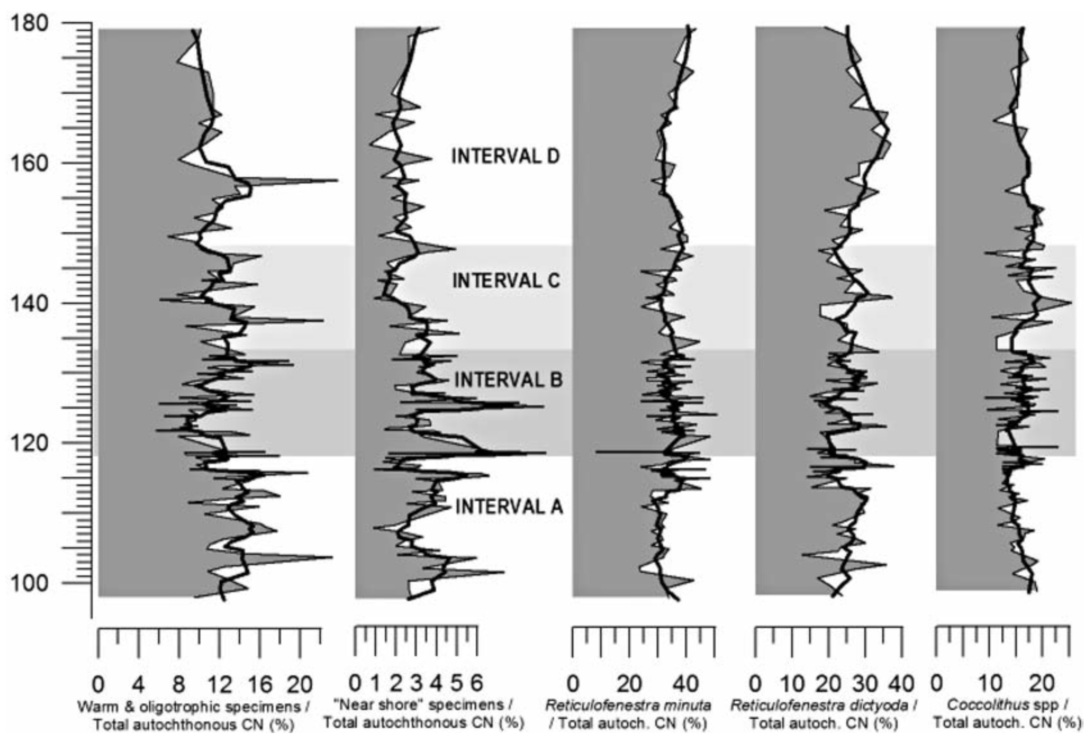


**Fig. 4.** Stratigraphic distribution and relative abundance of selected, environmentally significant autochthonous taxa (see Appendix 2 for quantitative data). The thick black curves show 5-point running mean values and illustrate general trends. Note that scale-bars are different for each case.

For paleoceological purposes, the most common taxa, such as *Reticulofenestra dictyoda*, *Reticulofenestra minuta* and *Coccolithus* spp., were counted in one round. However, a second round was completed in order to count less common but environmentally significant taxa, such as *Discoaster*, *Sphenolithus*, *Zygrhablithus*, *Chiasmolithus*, *Ericsonia*, *Neococcolithes*, *Pontosphaera*, *Helicosphaera*, *Lanternithus*, *Braarudosphaera*, *Micrantolithus* and *Pemma*. The percentage of paleoecologically significant taxa was calculated by dividing the number count of a given taxa by the total count of autochthonous specimens (Fig. 4). Given that all genera with similar paleoecological affinities showed the same trends throughout the succession, they were grouped and represented together (Fig. 4).

## 4. Results

### 4.1 Taxonomy and paleoecological significance

One hundred and thirty six taxa were found to be present in the Gorrondatxe samples (see Appendix 1), eighty-three of which were autochthonous, while fifty-three were reworked (Plate 1). *Reticulofenestra* made up ca. 60 % of the assemblage. Large specimens (more than 5 µm), the majority of which had a narrow central area, were classified as *Reticulofenestra dictyoda* and interpreted as cosmopolitan (Okada and Honjo 1973, Honjo 1976). Small reticulofenestrids (less than 5 µm) were attributed to *Reticulofenestra minuta*, which is generally interpreted as an r-type opportunistic taxon that blooms in upwelling zones (Hallock 1987, Flores et al. 1995). *Coccolithus* spp. is also abundant, but its paleoecological significance during the Eocene period is not clear (Aubry 1998, Bown et al. 2004).

*Discoaster* spp., *Sphenolithus* spp. and *Zygrhablithus bijugatus* are all considered warm and oligotrophic indicators (Garner and Bukry 1969, Prins 1971, Haq et al. 1977, Wei and Wise 1990, Aubry 1992, Bown et al. 2004). Their cumulative abundance was plotted as "warm and oligotrophic taxa" (Fig. 4).

*Pontosphaera* spp., *Helicosphaera* spp., *Braarudosphaera* spp., *Micrantolithus* spp., *Pemma* spp., *Pseudotriquetrorhabdulus inversus* and *Lanternithus* spp. are considered inhabitants of epicontinental areas, rather than of open oceans, and were able to adapt to conditions in which some seawater characteristics, such as salinity and continental input, changed (Haq and Lohman 1976, Wei and Wise 1990, Winter et al. 1994, Aubry 1998, Cachão et al. 2002, Khalil and Al Sawy 2014). Their cumulative abundance was represented as "near-shore taxa" (Fig. 4). The rest of the species identified (Appendix 1) constituted less than 1 % of the assemblage and were not considered relevant to the present study.

### 4.2 Stratigraphic variations in assemblages

Calcareous nannofossil preservation is generally medium to good in Gorrondatxe (Plate 1). However, some *Discoaster* and *Zygrhablithus bijugatus* specimens were found to be slightly re-crystallized. Although evidence of incipient dissolution was observed in some samples of Interval B, *Zygrhablithus bijugatus* and *Reticulofenestra minuta* are present throughout the succession (Fig. 3), showing that dissolution did not significantly modify the composition of the assemblages.

The stratigraphic distribution of the most significant taxa is shown in figures 3 and 4 (see details in Appendix 2 for quantitative data). The number of autochthonous calcareous nannofossils per mm$^2$ decreased significantly from an average value of ca. 3169 specimens/mm$^2$ in Interval A to an average of 2257 specimens/mm$^2$ in Interval B, at the core of the C21r-H6 event (118–133 m; Fig. 3). The quantity increased progressively across Interval C (average of ca. 3254 specimens/mm$^2$) and the initial 10 m of Interval D (ca. 4034 specimens/mm$^2$), and then decreased to ca. 2664 specimens/mm$^2$. Conversely, the proportion of reworked specimens (Fig. 3) increased from 16.08 % in Interval A to 20.92 % in Interval B (peaking at 40 % in some samples) and 19.18 % in Interval C, decreasing again in Interval D (11.33 %).

The proportion of the most common taxa remained relatively constant throughout the succession, but increased slightly towards the top of the section. *Reticulofenestra dictyoda* made up an average of 24.85 % in Interval A, 22.97 % in Interval B, 24.26 % in Interval C, and 27.94 % in Interval D (Fig. 4). *Reticulofenestra minuta* represented 32.22 % in Interval A, 34.93 % in Interval B, 33.8 % in Interval C and 35.31 % in Interval D. *Coccolithus* spp. constituted 15.35 % of the assemblage in Interval A, 15.58 % in Interval B, 17.09 % in Interval C and 16.35 % in Interval D.

Warm and oligotrophic water taxa (represented by *Discoaster* spp., *Sphenolithus* spp. and *Zygrhablithus bijugatus*) did not vary greatly within the C21r-H6 event (Fig. 4). They represented 13.7 % of the assemblage in Interval A, and slightly decreased to 11.56 %

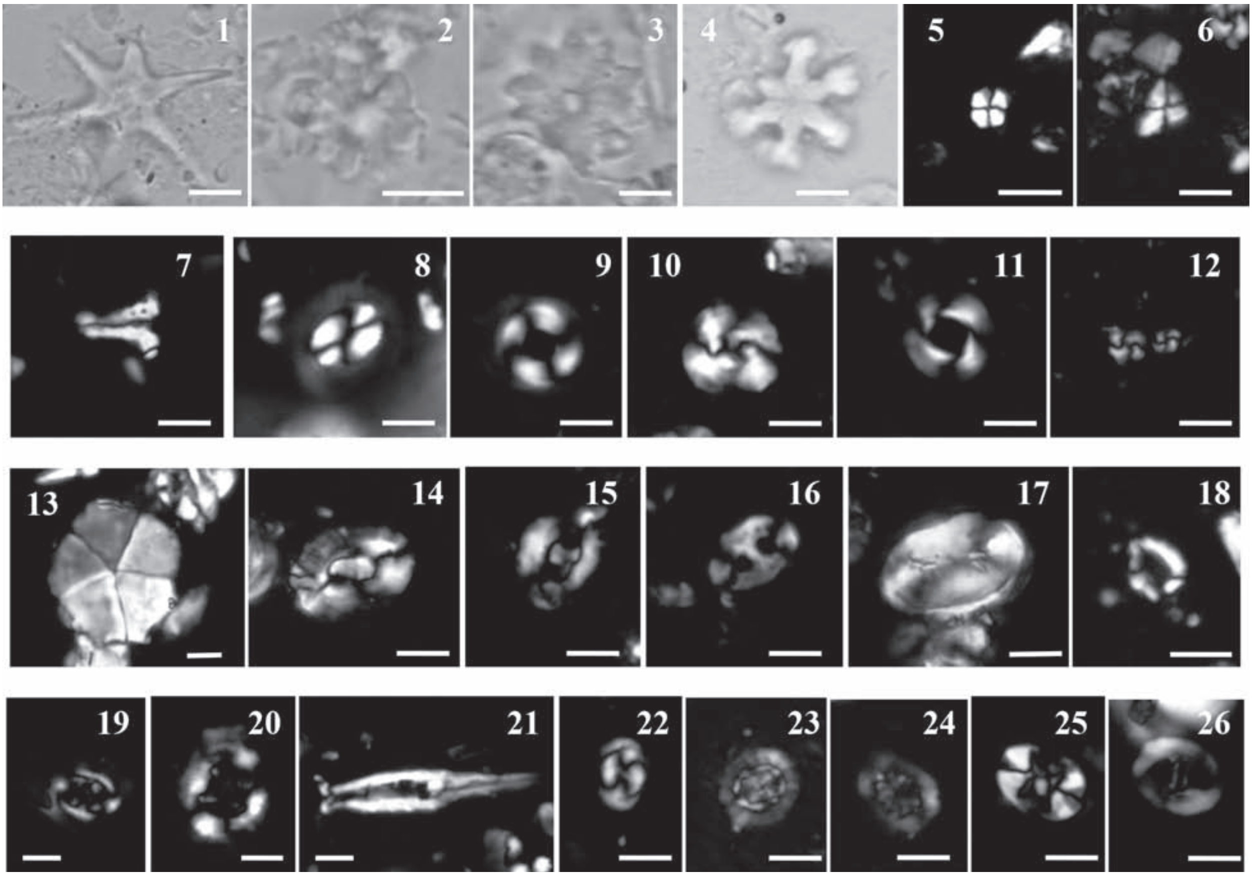

**Plate 1.** Microphotos of the most significant species found in the Gorrondatxe section. Scale bar 5 μm. **Autochthonous taxa:** (1) *Discoaster lodoensis*. (2) *Discoaster kuepperi*. (3) *Discoaster barbadiensis*. (4) *Discoaster deflandrei*. (5) *Sphenolithus moriformis*. (6) *Sphenolithus spiniger*. (7) *Zygrhablithus bijugatus*. (8) *Coccolithus pelagicus*. (9) *Coccolithus formosus*. (10) *Reticulofenestra dictyoda* with narrow central area. (11) *Reticulofenestra dictyoda* with wide central area. (12) *Reticulofenestra minuta* (13) *Braarudosphaera bigelowii*. (14) *Helicosphaera lophota*. (15) *Helicosphaera seminulum*. (16) *Pontosphaera pulchra*. (17) *Pontosphaera plana*. (18) *Lanternithus minutus*. (19) *Chiasmolithus solitus*. (20) *Chiasmolithus consuetus*. (21) *Blackites inflatus*. **Reworked taxa:** (22) *Toweius pertusus*. (23) *Prediscosphaera* sp. (24) *Cretarhabdus* sp. (25) *Eiffelithus* sp. (26) *Tranolithus* sp.

in Interval B, 12.03% in Interval C and 11.5% in Interval D. The average content in "near-shore" calcareous nannofossils increased slightly from 3.46% in Interval A to 4.04% in Interval B, and decreased to 2.49% in Interval C and 2.4% in Interval D. Interestingly, two significant peaks occurred within Interval B: the average value was 6.85% between 118 and 119 m (peaking at 9.37%), and 6.52% at 125–126 m (peaking at 9.27%).

Taking everything into account, the following five characteristics can be highlighted regarding the calcareous nannofossil assemblages of the C21r-H6 deposits in Gorrondatxe: i) the number of autochthonous calcareous nannofossil decreased; ii) the proportion of reworked specimens increased sharply; iii) the abundance of "near-shore" taxa showed two significant peaks; iv) the abundance of warm and oligotrophic taxa decreased slightly; v) the proportion of *Reticulofenestra dictyoda*, *Reticulofenestra minuta* and *Coccolithus* spp. taxa did not show any significant variation.

## 5. Discussion

### 5.1 Was the C21r-H6 event a hyperthermal?

Using benthic foraminiferal $\delta^{18}O$ data from the tropical western Atlantic ODP Site 1258, Sexton et al. (2011) concluded that the C21r-H6 event caused a 2 °C warming of bottom lying waters, leading to its classification as a hyperthermal event. This paleotemperature estimation could not be confirmed with oxygen isotope data from the Gorrondatxe section, as $\delta^{18}O$ values were affected by diagenetic alteration during burial (Payros et al. 2012). Despite this limitation, on the basis of an increase in the proportion of warm-water planktonic foraminifera throughout intervals B–C and the lowermost part of Interval D, warming of the Gorrondatxe sea-surface waters was deemed to be likely. However, warming over and above natural fluctuations could not be clearly demonstrated.

Similarly, the calcareous nannofossil data presented herein does not show any evidence of rising temperatures during the C21r-H6 event. Paleoecological interpretations derived from autochthonous taxa are not straightforward due to the high number of reworked specimens. However, it is significant that the abundance of warm and oligotrophic taxa did not increase within Intervals B and C, but rather decreased slightly. This suggests that temperature was not the main factor controlling the distribution of calcareous nannofossil assemblages in the Gorrondatxe area during the C21r-H6 event.

## 5.2 Integrated paleoecological interpretation

The most significant characteristics of the calcareous nannofossil assemblages found in the C21r-H6 deposits of Gorrondatxe are the decrease in autochthonous calcareous nannofossils per $mm^2$, the increase in reworked taxa, and the two prominent peaks of "near-shore" taxa. These characteristics strongly suggest that seaward-directed currents transported a large volume of reworked material into the ocean, including terrigenous sediments.

The increase in terrigenous sediment supply caused both a dilution of calcareous nannofossils and a reduction in the abundance of autochthonous calcareous nannofossils. A greater terrigenous influx was in all likelihood driven by increased supply of fluvial freshwater into the ocean. Changes in salinity and density in shallow seawaters could, in fact, be responsible for the two peaks in "near-shore" taxa found in Interval B. The low-density shallow water masses probably did not mix with deeper saline waters, leading to seawater stratification. As an additional consequence, the abundance of warm and oligotrophic taxa, which theoretically should increase during hyperthermal events, did not show significant variations across the C21r-H6 event.

Interestingly, previous data from the Gorrondatxe section demonstrated that continental input did increase during Interval B of the C21r-H6 event: trace fossil and benthic foraminifera data indicated greater input of refractory organic matter and plant detritus, whereas sedimentological data showed a greater abundance of turbidites, clays and kaolinite (Payros et al. 2012), which is commonly derived from (paleo)soils rich in iron (Chamley 1998).

The increased terrigenous sediment and freshwater input was related to the accelerated hydrological cycle, which intensified weathering and runoff on land. This scenario is similar to the models derived from other Eocene hyperthermal events (Barron et al. 1989, Schmitz and Pujalte 2003, Wing et al. 2005, Held and Soden 2006, Sluijs et al. 2009), some of which also concluded that the increased continental input boosted nutrient levels, leading to eutrophication of shallow seawaters (Bralower et al. 1995, Thompson and Schmitz 1997, McGonigal and Wise 2001, Taylor and Macquaker 2011). However, the Gorrondatxe data do not confirm seawater eutrophication, as small placoliths such as *Reticulofenestra minuta*, which become abundant in nutrient-rich environments, showed no significant variations. The cosmopolitan *Reticulofenestra dictyoda* did not show any variations either.

In conclusion, the calcareous nannofossil characteristics found at the C21r-H6 event can be attributed to the accelerated hydrological cycle on land and increased terrestrial input to the sea. Increased continental silicate weathering due to the accelerated hydrological cycle has been regarded as one of the main processes which consumes atmospheric $CO_2$ and drives seawater alkalinity (Jiang and Wise 2006, Agnini et al. 2009, Krishnan et al. 2014, Penman 2016). The resulting oceanic deposits are generally characterized by increased carbonate content and high $\delta^{13}C$ values (Ridgwell and Zeebe 2005, Stap et al. 2009), similar to those found in the lower part of Interval D of the Gorrondatxe section. Therefore, the combination of sedimentary, geochemical and calcareous nannofossil data from Gorrondatxe confirms the key role of continental silicate weathering in restoring pre-event environmental conditions.

## 5.3 Timing of the event

The sharp decrease in the abundance of autochthonous calcareous nannofossils and of warm and oligotrophic taxa at 115 m, 3 m below Interval B, suggests that some of the C21r-H6 environmental changes could

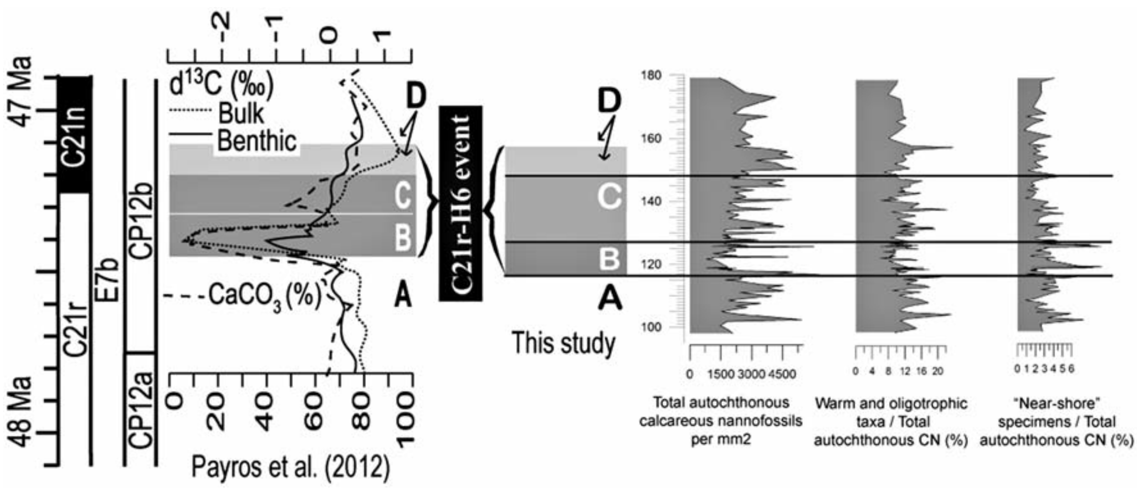

**Fig. 5.** Comparison of the initial subdivision of the C21r-H6 event in the Gorrondatxe section (left-hand side; Payros et al. 2012) and the updated subdivision derived from calcareous nannofossil data (right-hand side). The sea-surface perturbation began 32 kyr earlier than previously estimated (onset of Interval B) and was characterized by significant terrestrial input. Interval C represents the recovery phase, while Interval D corresponds to post-event deposits.

have started in the uppermost part of Interval A (Fig. 5). Interestingly, Payros et al. (2012) showed that the abrupt drop in $\delta^{13}C$ recorded in the lower part of Interval B was preceded by a gradual decline in the uppermost part of Interval A, along with a gradual decrease in the planktonic/benthic foraminiferal ratio, an increase in radiolarian abundance and a peak of the opportunistic benthic foraminifer *Aragonia aragonensis*. According to Payros et al. (2012), the uppermost 3 m of Interval A represent 1.5 precession cycles, which lasted approximately 32 kyr. In line with these observations, similar decreases in $\delta^{13}C$ and biotic perturbations also preceded the PETM, ETM2, ETM3 and H2 hyperthermal events by several 10s of kyr (Sexton et al. 2006, Nicolo et al. 2007, Stap et al. 2009, Alegret et al. 2010).

The abundance of autochthonous calcareous nannofossils, as well as that of warm and oligotrophic taxa, reached minimum values at 125 m, alongside a peak in abundance of "near-shore" taxa (Fig. 5). Payros et al. (2012) showed that the abundance of opportunistic benthic foraminifers also peaked at 125 m. Furthermore, this level corresponded to the inflexion point in the stable isotope record, showing minimum values (Fig. 2). These characteristics suggest that environmental conditions deteriorated progressively during the onset of the C21r-H6 event (115–125 m of Interval B), causing intensified warming, and accelerating the hydrological cycle and continental discharge to the sea.

The characteristics of the calcareous nannofossil assemblages gradually recovered from 125 m to 148 m (Fig. 5). This suggests that the environmental conditions began to return to pre-event levels in the upper part of Interval B (Payros et al. 2012), and continued improving throughout Interval C. The lowermost 10 m of Interval D corresponded to a transient overcompensation phase in which pre-event carbonate content and $\delta^{13}C$ were temporarily exceeded, thus resembling the aftermath of many hyperthermal events (Ridgwell and Zeebe 2005, Stap et al. 2009). All things considered, using the age model by Payros et al. (2012) the core of the C21r-H6 hyperthermal event lasted 80 kyr (115–125 m) and was followed by a longer recovery phase that lasted another 178 kyr (125–148 m).

## 6. Conclusions

Calcareous nannofossil assemblages of the Gorrondatxe area underwent significant changes during the C21r-H6 event. The abundance of autochthonous calcareous nannofossils decreased considerably during 80 kyr, whereas that of reworked specimens increased. However, the event did not cause drastic alterations in the composition of the autochthonous calcareous nannofossil assemblages. The abundance of warm and oligotrophic taxa decreased slightly and two prominent peaks of epicontinental taxa occurred. These characteristics, combined with a previously documented drop in $\delta^{13}C$ and an increase in the abundance of clay minerals, especially kaolinite, support a scenario with intensified continental input, similar to that suggested for other

Eocene hyperthermal events (e.g., PETM, ETM2, H2, ETM3). It can be therefore concluded that the accelerated hydrological cycle during the C21r-H6 event led to intensified weathering and runoff on land, increased continental sediment and fresh water supply to the sea, and possibly caused stratification of the water column. These interpretations support the hypothesis that increased silicate weathering led to a progressive reduction in atmospheric $CO_2$ levels during the 178 kyr of the recovery phase.

**Acknowledgements.** This research was funded by the Spanish Government project CGL2015-65404-R (MINECO/FEDER), and by the Basque Government project IT-930-16. BI-Z received a pre-doctoral grant from the University of the Basque Country (UPV/EHU). Thanks are due to Carl Sheaver for his language corrections and to the Oceanic Geoscience Group (GGO) from Salamanca for their help in calcareous nannofossil sample preparation and analysis. Earlier versions of this work benefitted from comments by reviewer Claudia Agnini and editor Joerg Pross.

## References

Adelseck, Jr., C.G., Geehan, G.W., Roth, P.H., 1973: Experimental evidence for the selective dissolution and overgrowth of calcareous nannofossils during diagenesis. Geological Society of America Bulletin 84, 2755–2762.

Agnini, C., Fornaciari, E., Rio, D., Tateo, F., Backman, J., Giusberti, L., 2007. Responses of calcareous nannofossil assemblages, mineralogy and geochemistry to the environmental perturbations across the Paleocene/Eocene boundary in the Venetian Pre-Alps. Marine Micropaleontology 63, 19–38.

Agnini, C., Macrì, P., Backman, J., Brinkhuis, H., Fornaciari, E., Giusberti, L., Luciani, V., Rio, D., Sluijs, A., Speranza, F., 2009. An early Eocene carbon cycle perturbation at ~52.5 Ma in the Southern Alps: Chronology and biotic response. Paleoceanography 24, 2209–2222.

Alegret, L., Ortiz, S., 2010. El corte de Zumaya (España): Registro de los foraminíferos bentónicos del Paleógeno inferior, Revista Mexicana de Ciencias Geológicas 27(3), 477–489.

Aubry, M.P., 1992. Late paleogene calcareous nannoplankton evolution: a tale of climatic deterioration. In: Prothero, D.R., Berggren, W.A. (Eds.), Eocene–Oligocene Climatic and Biotic Evolution. Princeton University Press, p. 272–309.

Aubry, M.P., 1998. Early Paleogene Calcareous nannoplankton evolution: a tale of climatic amelioration. In: Aubry, M.-P., Lucas, S., Berggren, W.A. (Eds.), Late Paleocene–early Eocene Biotic and Climatic Events in the Marine and Terrestrial Records. Columbia University Press, New York, p. 158–201.

Aubry, M.P., 2001. Provincialism in the photic zone during the LPTM. In: Ash, A.M., Wing, S.L. (Eds), Climate and Biota of the Early Paleogene, Internacional meeting, Wyoming, USA, p. 6.

Barron, E., Hay, W., Thompson, S., 1989. The hydrologic cycle: a major variable during Earth history. Palaeogeography, Palaeoclimatology, Palaeoecology 75, 157–174.

Bice, K.L., Marotzke, J., 2000. Warrn climate dynamics. GFF 122, 29–30.

Bown, P.R., Lees, J.A., Young, J.R., 2004. Calcareous nannoplankton evolution and biodiversity through time. In: Thierstein, H.R., Young, J.R. (Eds.), Coccolithophores: from molecular processes to global impact. Springer, New York, p. 481–508.

Bralower, T.J., Zachos, J.C., Thomas, E., Parrow, M., Paull, C.K., Kelly, D.C., Premoli Silva, I., Sliter, W.V., Lohmann, K.C., 1995. Late Paleocene to Eocene paleoceanography of the ecuatorial pacific ocean: Stables isotopes recorded at ODP Site 865, Allison Guyot. Paleoceanography 10, 841–865.

Bralower, T.J., 2002: Evidence of surface water oligotrophy during the Paleocene–Eocene Termal Maximum: Nannofossil assemblage data from ocean drilling program Site 690, Maud Rise, Weddell Sea. Paleoceanography 17(2), 1029–1042.

Cachão, M., Drago, T., Silva, A.D., Moita, T., Oliveira, A., Naughton, F., 2002. The secret (estuarine?) life of *Helicosphaera carteri*: Preliminary results. Journal of Nannoplankton Research 24, 76–77.

Chamley, H., 1998. Clay mineral sedimentation in the Ocean. In: Paquet, H., Clauer, N. (Eds.), Soil and sediments (mineralogy and geochemistry). Springer-Verlag, Berlin, p. 269–302. ODP Proceedings 108. Ocean Drill Program, College Station, Texas, p. 121–141.

Cramer, B.S., Wright, J.D., Kent, D.V., Aubry, M.P., 2003. Orbital climate forcing of $\delta^{13}C$ excursions in the late Paleocene–early Eocene (chrons C24n–C25n). Paleoceanography 18 (4), 1097–1117.

Dedert, M., Stoll, H.M., Kroon, D., Shimizu, N., Kanamaru, K., Ziveri, P., 2012. Productivity response of calcareous nannoplankton to Eocene Thermal Maximum 2 (ETM2). Climate of the Past 8, 977–993.

Dennison, J.M., Hay, W.W., 1967. Estimating the needed sampling area for subaquatic ecologic studies. Journal Paleontology 41, 706–708.

Dickens, G.R., O'Neil, J.R., Rea, D.K., Owen, R.M., 1995. Dissociation of oceanic methane hydrate as a cause of the carbon isotope excursion at the end of the Paleocene. Paleoceanography 10, 965–971.

Firth, J.V., Eldrett, J.S., Harding, I.C., Coxall, H.K., Wade, B.S., 2012: Palaeoceanographic events from high to low latitudes of ODP Hole 647A: implications for correlating Integrated biomagnetochronology for the Palaeogene. Geological Society, London, Special Publications, Vol. 373.

Flores, J.A., Sierro, F.J., Raffi, I., 1995. Evolution of the calcareous nannofossil assemblage as a response to the paleoceanographic changes in the eastern equatorial Pacific Ocean from 4 to 2 Ma, Leg 138, sites 849 and 852.

In: Pisias, N.G., Mayer, L.A., Janecek, T.R., Palmer-Julson, A., van Andel, T.H. (Eds.), Proceedings of the Ocean Drilling Program, Scientific Results 138. College Station, Texas, p. 163–176.

Flores, J.A., Sierro, F.J., 1997. Revised technique for calculation of calcareous nannofossil accumulation rates. Micropaleontology 43, 321–324.

Fuertes, M.A., Flores, J.A., Sierro, F.J., 2014: The use of circularly polarized light for biometry, identification and estimation of mass of coccoliths. Marine Micropaleontology, 113, 44–55.

Gartner Jr., S., Bukry, D., 1969. Tertiary holococcolith. Journal of Paleontology 43, 1213–1220.

Gibbs, S.J., Bralower, T.J., Bown, P.R., Zachos, J.C., Bybell, L.M., 2006. Shelf and open-ocean calcareous phytoplankton assemblages across the Paleocene–Eocene thermal maximum: implications for global productivity gradients. Geology 34 (4), 233–236.

Gibbs, S.J., Stoll, H.M., Bown, P.R., Bralower, T.J., 2010: Ocean acidification and surface water carbonate production across the Paleocene–Eocene thermal maximum. Earth and Planetary Science Letters 295, 583–592.

Giusberti, L., Rio, D., Agnini, C., Backman, J., Fornaciari, E., Tateo, F., Oddone, M., 2007. Mode and tempo of the Paleocene–Eocene thermal maximum in an expanded section from the Venetian pre-Alps. Geological Society of America Bulletin 119 (3–4), 391–412.

Hallock, P., 1987. Fluctuations in the trophic resource continuum: a factor in global diversity cycles? Paleoceanography 2 (5), 457–471.

Haq, B.U., Lohmann, G.P., 1976. Early Cenozoic calcareous nannoplankton biogeography of the Atlantic Ocean. Marine Micropaleontology 1, 119–194.

Haq, B.U., Premoli Silva, I., Lohmann, G.P., 1977. Calcareous plankton paleobiogeographic evidence for major climatic fluctuations in the Early Cenozoic Atlantic Ocean. Journarl of Geophysical Results 82, 3861–3876.

Held, I.M., Soden, B.J., 2006. Robust responses of the hydrological cycle to global warming. Journal Climate 19, 5686–5699.

Honjo, S., 1976. Coccoliths – production, transportation and sedimentation. Marine Micropaleontology 1, 65–79.

Huber, M., Sloan, L.C., 2000. Climatic responses to tropical sea surface temperature changes on a "greenhouse" Earth. Paleoceanography 15, 443–450.

Jiang, S., Wise Jr., S.W., 2006. Surface-water chemistry and fertility variations in the tropical Atlantic across the Paleocene/Eocene Thermal Maximum as evidenced by calcareous nannoplankton from ODP Leg 207, Hole 1259B. Revue de micropaléontologie 49, 227–244.

Kennett, J.P., Stott, L.D., 1991. Abrupt deep-sea warming, paleoceanographic changes and benthic extinctions. Nature 353, 225–229.

Khalil, H., Al Sawy, S., 2014. Integrated biostratigraphy, stage boundaries and Paleoclimatology of the Upper Cretaceous–Lower Eocene successions in Kharga and Dakhala Oases, Western Desert, Egypt. Journal of African Earth Sciences 96, 220–242.

Kirtland Turner, S., Sexton, P.F., Charles, C.D., Norris, R.D., 2014. Persistence of carbon release events through the peak of early Eocene global warmth. Nature Geoscience 7, 748–751.

Krishnan, S., Pagani, M., Huber, M., Sluijs, A., 2014. High latitude hydrological changes during the Eocene Thermal Maximum 2. Earth and Planetary Science Letters 404, 167–177.

Lourens, J.L., Sluijs, A., Kroon, D., Zachos, J.C., Thomas, E., Röhl, U., Bowles, J., Raffi, I., 2005. Astronomical pacing of late Paleocene to early Eocene global warming events. Nature 435, 1083–1087.

Masson-Delmotte, V., Schulz, M., 2013. Information from paleclimate archives. In: Stocker, T.F., Qin, D., Plattner, G.K., Tignor, M., Allen, S.K., Boschung, J., Nauels, A., Xia, Y., Bex, V., Midgley, P.M. (Eds.), Climate Change 2013: The Physical Science Basis. Contribution of Working Group I to the Fifth Assessment Report of the Intergovernmental Panel on Climate Change. Cambridge University Press, Cambridge, United Kingdom and New York, NY, USA. Chapter 5.

McGonigal, K.L., Wise, S.W. Jr., 2001. Eocene calcareous nannofossil biostratigraphy and sediment accumulation of turbidite sequences on the Iberia Abyssal Plain, ODP Sites 1067–1069. In: Beslier, M.O., Whitmarsh, R.B., Wallace, P.J., Girardeau, J. (Eds.), Proceedings ODP, Scientific Results 173, p. 1–35.

Molina, E., Alegret, L., Apellaniz, E., Bernaola, G., Caballero, F., Dinarès-Turell, Hardenbol, J., Heilmann-Clausen, C., Larrasoaña, J.C., Luterbacher, H., Monechi, S., Ortiz, S., Orue-Etxebarria, X., Payros, A., Pujalte, V., Rodríguez-Tovar, F.J., Toris, F., Tosquella, J., Uchman, A., 2011. The Global Stratotype Section and Point (GSSP) for the base of the Lutetian Stage at the Gorrondatxe section, Spain. Episodes 34 (2), 86–108.

Monechi, S., Angori, E., Von Salis, K., 2000. Calcareous nannofossil turnover around the Paleocene/Eocene transition at Alamedilla (southern Spain). Bulletin de la Société Géologique de France 171(4), 477–489.

Nicolo, M.J., Dickens, G.R., Hollis, C.J., Zachos, J.C., 2007. Multiple early Eocene hyperthermals: their sedimentary expression on the New Zealand continental margin and in the deep sea. Geology 35 (8), 699–702.

Okada, H., Honjo, S., 1973. The distribution of oceanic coccolithophorids in the Pacific. Deep Sea Results 20, 355–374.

Orue-Etxebarria, B., Bernaola, G., Baceta, J.I., Angori, E., Caballero, F., Monechi, S., Pujalte, V., Dinarès-Turell, J., Apellaniz, E., Payros, A., 2004. New constraints on the evolution of planktic foraminifers and calcareous nannofossils across the Paleocene–Eocene boundary interval: the Zumaia section revisited. Neues Jahrbuch für Geologie und Paläontologie, Abhandlungen 234, 223–259.

Payros, A., Orue-Etxebarria, X., Pujalte, V., 2006. Covarying sedimentary and biotic fluctuations in Lower–Middle Eocene Pyrenean deep-sea deposits: Palaeoenvironmental implications. Palaeogeography, Palaeoclimatology, Palaeoecology 234, 258–276.

Payros, A., Bernaola, G., Orue-Etxebarria, X., Dinarès-Turell, J., Tosquella, J., Apellaniz. E., 2007. Reassessment of the Early–Middle Eocene biomagnetochronology based on evidence from the Gorrondatxe section (Basque Country, western Pyrenees). Lethaia 40, 183–195.

Payros, A., Tosquella, J., Bernaola, G., Dinarès-Turell, J., Orue-Etxebarria, X., Pujalte, V., 2009. Filling the North European Early/Middle Eocene (Ypresian/Lutetian) boundary gap: Insights from the Pyrenean continental to deep-marine record. Palaeogeography, Palaeoclimatology, Palaeoecology 280, 313–332.

Payros, A., Ortiz, S., Alegret, L., Orue-Etxebarria, X., Apellaniz, E., Molina, E., 2012. An early Lutetian carbon-cycle perturbations: Insights from the Gorrondatxe section (western Pyrenees, Bay of Biscay). Paleoceanography 27, 2213–2226.

Payros, A., Martínez-Braceras, N., 2014. Orbital forcing in turbidite accumulation during the Eocene greenhouse interval. Sedimentology 61, 1411–1432.

Penman, D. E., 2016: Silicate weathering and North Atlantic silica burial during the Paleocene–Eocene Thermal Maximum. Geology Vol. 44 (9), 731–734.

Penman, D. E., Kirtland-Turner, S., Sexton, P. F. et al., 2016: An abyssal carbonate compensation depth overshoot in the aftermath of the Paleocene–Eocene Thermal Maximum. Nature Geoscience Vol. 9 (8), p. 575.

Perch-Nielsen, K., 1985. Cenozoic calcareous nannofossils. In: Bolli, H. M., Saunders, J. B., Perch-Nielsen, K. (Eds.), Plankton Stratigraphy. Cambridge University Press, Cambridge, p. 427–554.

Prins B., 1971. Speculations on relations, evolution, and stratigraphic distribution of discoasters. In: Farinacci, A. (Ed.), Proceedings of the II Planktonic Conference, Editoriale Tecnoscienza, Roma, p. 1017–1037.

Raffi, I., De Bernardi, B., 2008. Response of calcareous nannofossils to the Paleocene–Eocene Thermal Maximum: observations on composition, preservation and calcification in sediments from ODP Site 1263 (Walvis Ridge – SW Atlantic). Marine Micropaleontology 69, 119–138.

Raffi, I., Backman, J., Zachos, J. C., Sluijs, A., 2009. The response of calcareous nannofossil assemblages to the Paleocene Eocene Thermal Maximum at the Walvis Ridge in the South Atlantic. Marine Micropaleontology 70, 201–212.

Röhl, U., Westerhold, T., Monechi, S., Thomas, E., Zachos, J. C., Donner, B., 2005. The Third and Final Early Eocene Thermal Maximum: Characteristics, Timing and Mechanisms of the 'X' Event, GSA Annual Meeting 37. Geological Society of America, Salt Lake City, USA. 264 p.

Schmitz, B., Pujalte, V., Nuñez-Betelu, K., 2000. Climate and sea level perturbations during the Initial Eocene Thermal Maximum: evidence from siliciclastic units in the Basque Basin (Ermua, Zumaia and Trabakua Pass), northern Spain. Palaeogeography, Palaeoclimatology, Palaeoecology 165, 299–320.

Schmitz, B., Pujalte, V., 2003. Sea-level, humidity, and land-erosion records across the initial Eocene thermal maximum from a continental-marine transect in northern Spain. Geology 31 (8), 689–692.

Schneider, L. J., Bralower, T. J., Kump, L. R., 2011. Response of nannoplankton to early Eocene ocean destratification. Palaeogeography, Palaeoclimatology, Palaeoecology 310, 152–162.

Self-Trail, J. M., Powars, D. S., Watkins, D. K., Wandless, G. A., 2012. Calcareous nannofossil assemblage changes across the Paleocene–Eocene Thermal Maximum: Evidence from a shelf setting. Micropaleontology 92–93, 61–80.

Sexton, P. F., Wilson, P. A., Norris, R. D., 2006. Testing the Cenozoic multisite composite $\delta^{18}O$ and $\delta^{13}C$ curves: new monospecific Eocene records from a single locality, Demerara Rise (Ocean Drilling Program Leg 207). Paleoceanography 21, 2019–2035.

Sexton, P. F., Norris, R. D., Wilson, P. A., Pälike, H., Westerhold, T., Röhl, U., Bolton, C. T., Gibbs, S., 2011. Eocene global warming events driven by ventilation of oceanic dissolved organic carbon. Nature 471, 349–352.

Sluijs, A., Schouten, S., Donders, T. H., Schoon, P. L., Röhl, U., Reichart, G. J., Sangiorgi, F., Kim, J.-H., Sinninghe Damsté, J. S., Brinkhuis, H., 2009. Warm and wet conditions in the Arctic region during Eocene Thermal Maximum 2. Nature Geoscience 2, 777–780.

Smith, A. G., 1996. Cenozoic latitudes, positions and topography of the Iberian Peninsula. In: Friend, P. F., Dabrio, C. J. (Eds.), Tertiary basins of Spain: the stratigraphic record of crustal kinematics. Cambridge University Press, Cambridge, p. 6–8.

Stap, L., Sluijs, A., Thomas, E., Lourens, L., 2009. Patterns and magnitude of deep sea carbonate dissolution during Eocene Thermal Maximum 2 and H2, Walvis Ridge, South-Eastern Atlantic Ocean. Paleoceanography 24, 1211–1223.

Taylor, K. G., Macquaker, J. H. S., 2011. Iron minerals in marine sediments record chemical environments. Elements 7, 113–118.

Thomas, E., Zachos, J. C., 2000. Was the late Paleocene Thermal Maximum a unique event? GFF 122 (1), 169–170.

Thompson, E., Schmitz, E., 1997. Barium and the late Paleocene $\delta^{13}C$ maximum: Evidence of increased marine surface productivity. Paleoceanography 12, 239–254.

Tremolada, F., Bralower, T. J., 2004. Nannofossil assemblage fluctuations during the Paleocene–Eocene Thermal Maximum at Sites 213 (Indian Ocean) and 401 (North Atlantic Ocean): palaeoceanographic implications. Marine Micropaleontology 52, 107–116.

Villa, G., Fioroni, C., Pea, L., Bohaty, S., Persico, D, 2008. Middle Eocene–late Oligocene climate variability: Calcareous nannofossil response at Kerguelen Plateau, Site 748. Marine Micropaleontology 69, 173–192.

Wei, W., Wise, S. W., 1990. Biogeographic gradients of middle Eocene–Oligocene calcareous nannoplankton in the South Atlantic Ocean. Palaeogeography, Palaeoclimatology, Palaeoecology 79, 29–61.

Wing, S. L., Harrington, G. J., Smith, F. A., Bloch, J. I., Boyer, D. M., Freeman, K. H., 2005. Transient floral change and rapid global warming at the Paleocene–Eocene boundary. Science 310, 993–996.

Winter, A., Jordon, R. W., Roth, P. H., 1994. Biogeography of living coccolithophores in ocean waters. In: Winter, A., Siesser, W. G. (Eds.), Coccolithophores. Cambridge University Press, Cambridge, p. 161–177.

Zachos, J., Pagani, M., Sloan, L., Thomas, E., Billups, K., 2001. Trends, Rhythms, and Aberrations in Global Climate 65 Ma to Present. Science 292, 686–693.

Zachos, J. C., Kroon, D., and 25 others, 2004. Early Cenozoic extreme climates: The Walvis Ridge transect: Proceedings of the Ocean Drilling Program, Leg 208.

Zachos, J., Dickens, G. R., Zeebe, R.E, 2008. An early Cenozoic perspective on greenhouse warming and carbon-cycle dynamics. Nature 451, 279–293.

Manuscript received: December 14, 2015
Revised version accepted: December 5, 2016

# Appendix 1

Taxonomic list of the taxa present in Gorrondatxe. For each autochthonous taxon (alphabetically ordered) we add: (i) the reference of the author that described it. (ii) The temporal constraint of the taxon, in which we have based the hypothesis that the taxon is autochthonous. (iii) Reference of the author who published such temporal constraint. For each reworked taxon (alphabetically ordered) we do not add points (ii) and (iii) due to their clearly reworked status.

## AUTOCHTHONOUS TAXA

| TAXON | CITATION | STRATIGRAPHIC RANGE | SOURCE OF STRAT. RANGE |
|---|---|---|---|
| ***Blackites*** | **Hay and Towe 1962** | | |
| *Blackites gladius* | (Locker 1967) Varol 1989 | NP14 (49.11 Ma) – NP15 (42.8 Ma) | Bown 2005, Perch-Nielsen 1985 |
| *Blackites inflatus* | (Bramlette and Sullivan 1961) Kapellos and Schaub 1973 | NP14b (47.84 Ma) – NP15a (45.49 Ma) | Perch-Nielsen 1985 |
| *Blackites perlongus* | (Deflandre 1952) Shafik 1981 | NP9 (57.21 Ma) – NP21 (32.92 Ma) | Bown 2005 |
| *Blackites spinosus* | (Deflandre in Deflandre and Fert 1954) Hay and Towe 1962 | NP14b (47.84 Ma) – NP23 (29.62 Ma) | Bown 2005 |
| ***Braarudosphaera*** | **Deflandre 1947** | | |
| *Braarudosphaera bigelowii* | (Gran and Braarud 1935) Deflandre 1947 | Cenomanian (100.5 Ma) – Extant | Burnett 1998, Young et al. 2003 |
| *Brarudosphaera perampla* | Bown 2010 | NP6 (59.54 Ma) – NP23 (29.62 Ma) | Bown 2010 |
| *Braarudosphaera sequela* | Self-Trail 2011 | NP6 (59.54 Ma) – NP23 (29.62 Ma) | Nannotax rough estimate |
| ***Calcidiscus*** | Kamptner 1950 | | |
| *Calcidiscus bicircus* | Bown 2005 | NP12 (53.7 Ma) – NP17 (37.32 Ma) | Shamrock & Watkins 2008, Bown et al. 2007 |
| *Calcidiscus pacificanus* | (Bukry 1971) Varol 1989 | NP10 (55.85 Ma) – NP17 (37.32 Ma) | Shamrock & Watkins 2008 |
| ***Camplosphaera*** | **Kamptner 1963** | | |
| *Campylosphaera dela* | (Bramlette & Sullivan, 1961) Hay & Mohler, 1967 | NP6 (59.54 Ma) – NP17 (37.32 Ma) | Nannotax rough estimate |
| ***Chiasmolithus*** | **Hay et al. 1966** | | |
| *Chiasmolithus consuetus* | (Bramlette and Sullivan 1961) Hay and Mohler 1967 | NP5 (61.51 Ma) – NP16 (40.4 Ma) | Perch-Nielsen 1985 |
| *Chiasmolithus grandis* | (Bramlette and Riedel 1954) Radomski 1968 | NP11 (54.17 Ma) – NP 17 (37.32 Ma) | Perch-Nielsen 1985 |
| *Chiasmolithus nitidus* | Perch-Nielsen 1971 | NP6 (59.54 Ma) – NP21 (32.92 Ma) | Nannotax rough estimate |
| *Chiasmolithus solitus* | (Bramlette and Sullivan 1961) Locker 1968 | NP9 (57.21 Ma) – NP16 (40.4 Ma) | Perch-Nielsen 1985 |
| ***Clathrolithus*** | **Deflandre in Deflandre and Fert 1954** | | |
| *Clathrolithus ellipticus* | Deflandre in Deflandre and Fert 1954 | NP6 (59.54 Ma) – NP16 (40.4 Ma) | Nannotax rough estimate |
| ***Clausicoccus*** | **Prins 1979** | | |
| *Clausicoccus fenestratus* | (Deflandre and Fert 1954) Prins 1979 | NP12 (53.7 Ma) – NN1 (22.82 Ma) | Self-Trail via comment, Young 1998 |
| *Clausicoccus subdistichus* | (Roth and Hay in Hay et al. 1967) Prins 1979 | NP14 (49.11 Ma) – NN2 (18.28 Ma) | Nannotax rough estimate |
| ***Coccolithus*** | **Schwartz 1894** | | |
| *Coccolithus biparteoperculatus* | (Varol 1991) Bown and Dunkley Jones 2012 | NP12 (53.7 Ma) – NP23 (29.62 Ma) | Varol 1991 |
| *Coccolithus cachaoi* | Bown 2005 | NP14 (49.11 Ma) – NP21 (32.92 Ma) | Bown, 2005 |
| *Coccolithus eopelagicus* | (Bramlette and Riedel 1954) Bramlette and Sullivan 1961 | NP14 (49.11 Ma) – NP23 (29.62 Ma) | Nannotax rough estimate |
| *Coccolithus formosus* | (Kamptner 1963) Wise 1973 | NP12 (53.7 Ma) – NP21 (32.92 Ma) | Perch-Nielsen 1985 |
| *Coccolithus mutatus* | (Perch-Nielsen 1971) Bown 2005 | NP15 (49.11 Ma) – NP15 (42.87 Ma) | Nannotax rough estimate |
| *Coccolithus pauxillus* | Bown 2010 | NP9 (57.21) – NP15 (42.87) | Bown, 2005 |
| *Coccolithus pelagicus* | (Wallich 1877) Schiller 1930 | Lower NP2 – Extant | Varol 1989, Young et al. 2003 |
| *Coccolithus staurion* | Bramlette and Sullivan 1961 | NP9 (57.21) – NP15 (42.87) | Perch-Nielsen 1985 |
| ***Cruciplacolithus*** | **Hay and Mohler in Hay et al. 1967** | Danian (66.04 Ma) – Extant | Nannotax rough estimate |
| ***Cyclicargolithus*** | **Bukry 1971** | NP9 (57.21 Ma) – NN6 (12.1 Ma) | Shamrock & Watkins 2008, Raffi et al. 2006 |
| ***Daktylethra*** | **Gartner in Gartner and Bukry 1969** | NP14b (47.82 Ma) – NP17 (37.32 Ma) | Bown & Dunkley Jones 2006 |
| ***Discoaster*** | **Tan 1927** | | |
| *Discoaster barbadiensis* | Tan 1927 | NP11 (54.17 Ma) – NP20 (34.44 Ma) | Nannotax rough estimate |
| *Discoaster deflandrei* | Bramlette and Riedel 1954 | NP13 (50.5 Ma) – NN7 (10.89 Ma) | Theodoridis 1984, Young 1998 |
| *Discoaster kuepperi* | Stradner 1959 | NP11 (54.17 Ma) – NP14 (46.29 Ma) | Nannotax rough estimate |
| *Discoaster lodoensis* | Bramlette and Sullivan 1961 | NP12 (53.7 Ma) – NP14 (46.29 Ma) | Perch-Nielsen 1985, Nannotax rough estimate |
| *Discoaster nodifer* | (Bramlette and Riedel 1954) Bukry 1973 | NP14 (49.11 Ma) – NP23 (29.62 Ma) | Nannotax rough estimate |
| *Discoaster saipanensis* | Bramlette and Riedel 1954 | NP14 (49.11 Ma) – NP20 (34.44 Ma) | Perch-Nielsen 1985 |
| *Discoaster sublodoensis* | Bramlette and Sullivan 1961 | NP14 (49.11 Ma) – NP15 (42.87 Ma) | Perch-Nielsen 1985 |
| *Discoaster wemmelensis* | Achuthan and Stradner 1969 | NP14 (49.11 Ma) – NP16 (40.4 Ma) | Nannotax rough estimate |
| ***Ericsonia*** | **Black (1964)** | | |
| *Ericsonia robusta* | (Bramlette and Sullivan 1961) Edwards and Perch-Nielsen 1975 | NP4 (63.25 Ma) – NP19 (34.44 Ma) | Bown & Dunkley Jones 2012 |
| ***Helicosphaera*** | **Kamptner 1954** | | |
| *Helicosphaera lophota* | (Bramlette and Sullivan 1961) Locker 1973 | NP12 (53.7 Ma) – NP18 (36.87 Ma) | Perch-Nielsen 1985 |
| *Helicosphaera seminulum* | Bramlette and Sullivan 1961 | NP12 (53.7 Ma) – NP16 (40.4 Ma) | Perch-Nielsen 1985 |
| ***Holodiscolithus*** | **Roth 1970** | | |
| *Holodiscolithus geisenii* | Bown 2005 | NP9 (57.21 Ma) – NP23 (29.62 Ma) | Bown & Dunkley Jones 2006 |

| TAXON | CITATION | STRATIGRAPHIC RANGE | SOURCE OF STRAT. RANGE |
|---|---|---|---|
| *Holodiscolithus macroporus* | (Deflandre in Deflandre and Fert 1954) Roth 1970 | NP9 (57.21 Ma) – NN20 (0.29 Ma) | Dunkley Jones et al. 2009 |
| *Holodiscolithus solidus* | (Deflandre in Deflandre and Fert 1954) Roth 1970 | NP4 (63.25 Ma) – NP23 (29.62 Ma) | Dunkley Jones et al. 2009 |
| ***Lanternithus*** | **Stradner 1962** | | |
| *Lanternithus minutus* | Stradner 1962 | NP14b (47.82 Ma) – NP23 (29.62 Ma) | Bown 2005 |
| *Lanternithus simplex* | Bown 2005 | NP6 (59.54 Ma) – NP15a (45.49 Ma) | Bown 2005 |
| ***Lophodolithus*** | **Deflandre in Deflandre and Fert 1954** | Selandian (61.61 Ma) – Bartonian (37.32 Ma) | Perch-Nielsen 1985 |
| ***Markalius*** | **Bramlette and Martini 1964** | | |
| *Markalius apertus* | Perch-Nielsen 1979 | NP1 (66.04 Ma) – NP16 (40.4 Ma) | Neptune records, Self-Trail 2011 |
| *Markalius inversus* | (Deflandre in Deflandre and Fert 1954) Bramlette and Martini 1964 | Campanian (83.64 Ma) – NP21 (32.92 Ma) | Burnett 1998, Neptune records |
| ***Micrantholithus*** | **(Deflandre in Deflandre and Fert 1954)** | | |
| *Micrantholithus astrum* | Bown 2005 | NP5 (61.51 Ma) – NP21 (32.92 Ma) | Nannotax rough estimate |
| *Micrantholithus flos* | (Deflandre in Deflandre and Fert 1954) | NP6 (59.54 Ma) – NP23 (29.62 Ma) | Bown 2005 |
| *Micrantholithus hebecupsis* | Bown 2005 | NP11 (54.17 Ma) – NP21 (32.92 Ma) | Bown 2005, Dunkley Jones et al. 2009 |
| ***Nannotetrina*** | **Achuthan and Stradner 1969** | | |
| *Nannotetrina cristata* | (Martini 1958) Perch-Nielsen 1971 | NP14b (47.82 Ma) – NP16 (40.4 Ma) | Perch-Nielsen 1985 |
| ***Neococcolithes*** | **Sujkowski 1931** | | |
| *Neococcolithes dubius* | (Deflandre in Deflandre and Fert 1954) Black 1967 | NP11 (54.17 Ma) – NP18 (36.97 Ma) | Shamrock & Watkins 2008, Perch-Nielsen 1985 |
| *Neococcolithes minutus* | (Perch-Nielsen 1967) Perch-Nielsen 1971 | NP14 (49.11 Ma) – NP20 (34.44 Ma) | Perch-Nielsen 1985 |
| *Neococcolithes nudus* | Perch-Nielsen 1971 | NP14 (49.11 Ma) – NP16 (40.4 Ma) | Perch-Nielsen 1985 |
| *Neococcolithes protenus* | (Bramlette and Sullivan 1961) Black 1967 | NP4 (63.25 Ma) – NP14 (46.29 Ma) | Perch-Nielsen 1985 |
| ***Pemma*** | **Klumpp 1953** | NP14b (47.82 Ma) – NP21 (32.92 Ma) | Dunkley Jones et al. 2009 |
| ***Pontosphaera*** | **Lohmann 1902** | | |
| *Pontosphaera duocava* | (Bramlette and Sullivan 1961) Romein 1979 | NP11 (54.17 Ma) – NP17 (37.32 Ma) | Nannotax rough estimate |
| *Pontosphaera exilis* | (Bramlette and Sullivan 1961) Romein 1979 | NP9 (57.21 Ma) – NP17 (37.32 Ma) | Bown 2005 |
| *Pontosphaera formosa* | (Bukry and Bramlette 1969) Romein 1979 | NP14 (49.11 Ma) – NP21 (32.92 Ma) | Nannotax rough estimate |
| *Pontosphaera multipora* | (Kamptner 1948 ex Deflandre in Deflandre and Fer 1954) Roth 1970 | Eocene (55.96 Ma) – Extant | Young et al. 2003 |
| *Pontosphaera pectinata* | (Bramlette and Sullivan 1961) Sherwood 1974 | NP14 (49.11 Ma) – NP17 (37.32 Ma) | Bown 2005 |
| *Pontosphaera plana* | (Bramlette and Sullivan 1961) Haq 1971 | NP9 (57.21 Ma) – NP23 (29.62 Ma) | Bown 2005 |
| *Pontosphaera pulcheroides* | (Sullivan 1964) Romein 1979 | NP12 (53.7 Ma) – NP16 (40.4 Ma) | Self-Trail 2011 |
| *Pontosphaera pulchra* | (Deflandre in Deflandre and Fert 1954) Romein 1979 | NP9 (57.21 Ma) – NP16 (40.4 Ma) | Self-Trail 2011 |
| *Pontosphaera pygmaea* | (Locker 1967) Bystricka and Lehotayova 1974 | NP12 (53.21 Ma) – Oligocene (23.02 Ma) | Self-Trail 2011 |
| ***Pseudotriquetror-habdulus*** | **Wise in Wise and Constans 1976** | | |
| *Pseudotriquetror-habdulus inversus* | (Bukry and Bramlette 1969) Wise in Wise and Constans 1976 | NP14b (47.82 Ma) – NP16 (40.4 Ma) | Nannotax rough estimate |
| ***Rhabdosphaera*** | **Haeckel 1894** | NP14 (49.11 Ma) – Extant | Bown 2005 |
| ***Reticulofenestra*** | **Hay et al. 1966** | | |
| *Reticulofenestra dictyoda* | Deflandre in Deflandre and Fert 1954 | NP13 zone (50.50 Ma) – Oligocene (23.03) | Perch-Nielsen 1985 |
| *Reticulofenestra minuta* | Roth 1970 | NP13 zone (50.50 Ma) – Pliocene (2.59 Ma) | Young 1998 |
| ***Sphenolithus*** | **Deflandre in Grasse, 1952** | | |
| *Sphenolithus moriformis* | (Bronnimann and Stradner 1960) Bramlette and Wilcoxon 1967 | Selandian (61.61 Ma) – NN10 (8.29 Ma) | Agnini et al. 2007, Young 1998 |
| *Sphenolithus orphanknollensis* | Perch-Nielsen 1971 | NP11 (54.1 Ma) – NP15 (42.87 Ma) | Agnini et al. 2007, Perch-Nielsen 1985 |
| *Sphenolithus radians* | Defandre in Grasse 1952 | NP11 (54.2 Ma) – NP23 (29.62 Ma) | Agnini et al. 2007, Bown & Dunkley Jones 2012 |
| *Sphenolithus spiniger* | Bukry 1971 | NP14 (49.11 Ma) – NP17 (37.32 Ma) | Perch-Nielsen 1985, Fornaciari et al. 2010 |
| ***Toweius*** | **Hay and Mohler 1967** | | |
| *Toweius gammation* | Romein 1979 | NP11 zone (54.17 Ma) – NP 14 zone (46.29) | Perch-Nielsen 1985 |
| *Toweius magnicrassus* | (Bukry 1971) Romein 1979 | NP11 zone (54.17 Ma) – NP 14 zone (46.29) | Perch-Nielsen 1985 |
| ***Umbilicosphaera*** | **Lohmann 1902** | | |
| *Umbilicosphaera bramlettei* | (Hay and Towe 1962) Bown et al. 2007 | NP6 (59.54 Ma) – NP21 (32.92 Ma) | Bown et al. 2007 |
| *Umbilicosphaera jordanii* | Bown 2005 | NP4 (63.25 Ma) – NP23 (29.62 Ma) | Bown et al. 2007 |
| *Umbilicosphaera protoannulus* | (Gartner 1971) Young and Bown 2014 | NP11 (54.17 Ma) – NP21 (32.92 Ma) | Bown et al. 2007 |
| ***Zygrhablithus*** | **Deflandre 1959** | | |
| *Zygrhablithus bijugatus* | (Deflandre in Deflandre and Fert 1954) Deflandre 1959 | NP9 (57.21 Ma) – NN1 (22.82 Ma) | Agnini et al. 2007, Young 1998 |

## CENOZOIC REWORKED TAXA

| TAXON | CITATION |
|---|---|
| ***Calciosolenia*** | **Kamptner 1927** |
| ***Craticulithus*** | **Bown 2010** |
| ***Discoaster*** | **Tan 1927** |
| *Discoaster multiradiatus* | Bramlette and Riedel 1954 |
| ***Ellipsolithus*** | **Sullivan 1964** |
| ***Fasciculithus*** | **Bramlette and Sullivan 1961** |
| ***Heliolithus*** | **Bramlette and Sullivan 1961** |
| ***Hornibrookina*** | **Edwards 1973** |
| ***Neochiastozygus*** | **Perch-Nielsen 1971** |
| ***Prinsius*** | **Hay and Mohler 1967** |
| ***Toweius*** | **Hay and Mohler 1967** |
| *Toweius callosus* | Perch-Nielsen 1971 |
| *Toweius pertusus* | (Sullivan 1965) Romein 1979 |
| ***Tribrachiatus*** | **Shamrai 1963** |
| ***Zygodiscus*** | **Bramlette and Sullivan 1961** |

## MESOZOIC REWORKED TAXA

| TAXON | CITATION |
|---|---|
| *Ahmuellerella* | Reinhardt 1964 |
| *Amphizygus* | Bukry 1969 |
| *Arkhangelskiella* | Bekshina 1959 |
| *Braloweria* | Crux 1991 |
| *Broisonia* | Bukry 1969 |
| *Bukrylithus* | Black 1971 |
| *Calculites* | Prins and Sissingh in Sissingh 1977 |
| *Chiastozygus* | Gartner 1968 |
| *Crepidolithus* | Noël 1965 |
| *Cretarhabdus* | Bramlette and Martini 1964 |
| *Cribrosphaerella* | Deflandre in Piveteau 1952 |
| *Diadorhombus* | Worsley 1971 |
| *Eiffelithus* | Reinhardt 1965 |
| *Eprolithus* | Stover 1966 |
| *Gorkaea* | Varol and Girgis 1994 |
| *Helicolithus* | Noël 1970 |
| *Heteromarginatus* | Bukry 1969 |
| *Jakubowskia* | Varol 1989 |
| *Liliasterites* | Stradner and Steinmetz 1984 |
| *Loxolithus* | Noël 1965 |
| *Manivitella* | Thierstein 1971 |
| *Microrhabdulus* | Deflandre 1959 |
| *Micula* | Vekshina 1959 |
| *Munarinus* | Risatti 1973 |
| *Neocrepidolithus* | Romein 1979 |
| *Octolithus* | Romein 1979 |
| *Placozygus* | Hoffman 1970 |
| *Prediscosphaera* | Vekshina 1959 |
| *Quadrum* | Prins and Perch-Nielsen in Manivit et al. 1977 |
| *Radiolithus* | Stover 1966 |
| *Reinhardtites* | Perch-Nielsen 1968 |
| *Retecapsa* | Black 1971 |
| *Rhagodiscus* | Reinhardt 1967 |
| *Russellia* | Risatti 1973 |
| *Tranolithus* | Stover 1966 |
| *Tubirhabdus* | Rood et al. 1973 |
| *Watznaueria* | Reinhardt 1964 |
| *Zeugrhabdotus* | Reinhardt 1965 |

# Appendix 2

Abundance (raw values and percentage) of all calcareous nannofossil groups presented in the figures. Raw values were obtained by counting at least 500 specimens per smear slide. The total quantity of specimens counted per smear slide can be found in the last part of the table. Proportions were calculated by dividing the raw value of each autochthonous genus with the total amount of autochthonous specimens. Proportions of reworked specimens were calculated by dividing the raw value with the total amount of specimens (autochthonous + reworked). Grey background highlights samples collected within the C21r-H6 event interval.

| | | | REWORKED SPECIMENS | | MESOZOIC REWORKED | | CENOZOIC REWORKED | | |
|---|---|---|---|---|---|---|---|---|---|
| SAMPLE | Stratigraphic position (m) | Autochthonous specimens per mm$^2$ | Raw value | Percentage per total amount of specimens | Raw value | % total specimens | Raw value | % total specimens | Total counted specimens in first round |
| **GO-LU-156** | 179.2 | 1424 | 54 | 10.51 | 35 | 6.81 | 19 | 3.70 | 514 |
| **GO-LU-155** | 177.9 | 1850 | 69 | 12.99 | 37 | 6.97 | 32 | 6.03 | 531 |
| **GO-LU-154** | 174.5 | 2683 | 88 | 16.87 | 43 | 8.25 | 45 | 8.63 | 522 |
| **GO-LU-153** | 173 | 4196 | 54 | 9.79 | 30 | 5.49 | 24 | 4.30 | 547 |
| **GO-LU-152** | 169.8 | 2587 | 69 | 13.14 | 37 | 7.05 | 32 | 6.10 | 525 |
| **GO-LU-151** | 167.8 | 2135 | 96 | 17.87 | 65 | 12.16 | 31 | 5.71 | 535 |
| **GO-LU-150** | 166.9 | 3794 | 50 | 9.07 | 30 | 5.44 | 20 | 3.63 | 552 |
| **GO-LU-149** | 165.75 | 2735 | 39 | 7.49 | 20 | 3.84 | 19 | 3.65 | 521 |
| **GO-LU-148** | 164.5 | 2684 | 61 | 11.42 | 34 | 6.37 | 27 | 5.06 | 534 |
| **GO-LU-147** | 162.5 | 2420 | 46 | 8.46 | 28 | 5.15 | 18 | 3.31 | 544 |
| **GO-LU-146b** | 160.5 | 3078 | 43 | 8.59 | 28 | 5.56 | 15 | 3.03 | 495 |
| **GO-LU-146a** | 159.75 | 2566 | 40 | 7.55 | 21 | 3.96 | 19 | 3.58 | 530 |
| **GO-LU-145** | 158 | 2959 | 39 | 7.54 | 21 | 4.06 | 18 | 3.48 | 517 |
| **GO-LU-144b** | 157.5 | 2187 | 38 | 6.88 | 19 | 3.44 | 19 | 3.44 | 552 |
| **GO-LU-144a** | 156.7 | 3692 | 50 | 9.29 | 36 | 6.69 | 14 | 2.60 | 538 |
| **GO-LU-143b** | 155.65 | 4752 | 36 | 6.86 | 14 | 2.67 | 22 | 4.19 | 525 |
| **GO-LU-143a** | 154.9 | 4362 | 39 | 7.07 | 19 | 3.45 | 20 | 3.63 | 552 |
| **GO-LU-142b** | 153.75 | 5027 | 53 | 10.69 | 19 | 3.83 | 34 | 6.85 | 496 |
| **GO-LU-142a** | 153 | 3208 | 118 | 22.08 | 58 | 10.85 | 60 | 11.23 | 535 |
| **GO-LU-141** | 152.25 | 4115 | 77 | 13.74 | 38 | 6.78 | 39 | 6.96 | 561 |
| **GO-LU-140b** | 150.75 | 4647 | 54 | 9.00 | 34 | 5.67 | 20 | 3.33 | 600 |
| **GO-LU-140a** | 150.25 | 5169 | 62 | 11.98 | 35 | 6.76 | 27 | 5.22 | 518 |
| **GO-LU-139** | 149.6 | 2490 | 68 | 12.51 | 42 | 7.73 | 26 | 4.78 | 544 |
| **GO-LU-138** | 148.75 | 2880 | 103 | 19.58 | 60 | 11.41 | 43 | 8.17 | 526 |
| **GO-LU-137b** | 147.75 | 2454 | 148 | 27.23 | 102 | 18.77 | 46 | 8.46 | 544 |
| **GO-LU-137a** | 147.25 | 2031 | 130 | 22.51 | 75 | 12.99 | 55 | 9.52 | 578 |
| **GO-LU-30** | 146.75 | 4570 | 135 | 11.17 | 66 | 5.46 | 69 | 5.71 | 1209 |
| **GO-LU-136** | 145.75 | 3798 | 139 | 26.18 | 110 | 20.70 | 29 | 5.48 | 529 |
| **GO-LU-29** | 144.75 | 4643 | 121 | 9.98 | 38 | 3.14 | 83 | 6.85 | 1212 |
| **GO-LU-135** | 144.5 | 1963 | 178 | 33.97 | 134 | 25.57 | 44 | 8.40 | 524 |
| **GO-LU-28** | 143.5 | 3132 | 96 | 17.27 | 41 | 7.37 | 55 | 9.89 | 556 |
| **GO-LU-134** | 143.25 | 2761 | 101 | 21.67 | 54 | 11.59 | 47 | 10.09 | 466 |
| **GO-LU-Z** | 142.75 | 2190 | 117 | 23.26 | 73 | 14.51 | 44 | 8.75 | 503 |
| **GO-LU-27** | 141.25 | 2748 | 193 | 20.99 | 108 | 11.75 | 85 | 9.24 | 920 |
| **GO-LU-Y** | 140.75 | 2111 | 99 | 18.57 | 64 | 12.01 | 35 | 6.57 | 533 |
| **GO-LU-133** | 140.5 | 4931 | 46 | 8.32 | 14 | 2.53 | 32 | 5.79 | 553 |
| **GO-LU-132** | 139.5 | 1893 | 164 | 31.21 | 95 | 18.08 | 69 | 13.13 | 526 |
| **GO-LU-131** | 138 | 2428 | 87 | 16.89 | 57 | 11.07 | 30 | 5.83 | 515 |
| **GO-LU-26** | 137.5 | 4023 | 98 | 8.89 | 40 | 3.63 | 58 | 5.26 | 1103 |
| **GO-LU-130** | 136.75 | 1758 | 99 | 19.34 | 68 | 13.28 | 31 | 6.05 | 512 |
| **GO-LU-25** | 135.75 | 2339 | 155 | 17.68 | 87 | 9.93 | 68 | 7.76 | 877 |
| **GO-LU-X** | 135.5 | 2360 | 80 | 16.13 | 52 | 10.48 | 28 | 5.65 | 496 |
| **GO-LU-129** | 134.5 | 1889 | 65 | 12.77 | 41 | 8.06 | 24 | 4.72 | 509 |
| **GO-LU-24** | 132.75 | 4065 | 41 | 6.43 | 9 | 1.41 | 32 | 5.02 | 638 |
| **GO-LU-128** | 132.5 | 3413 | 86 | 17.66 | 53 | 10.88 | 33 | 6.78 | 487 |
| **GO-LU-V** | 132.25 | 4221 | 82 | 15.89 | 55 | 10.66 | 27 | 5.23 | 516 |
| **GO-LU-23** | 132 | 4576 | 101 | 9.69 | 36 | 3.45 | 65 | 6.24 | 1042 |
| **GO-LU-127** | 131.75 | 4324 | 45 | 8.14 | 24 | 4.34 | 21 | 3.80 | 553 |
| **GO-LU-U** | 131.5 | 2457 | 105 | 20.92 | 66 | 13.15 | 39 | 7.77 | 502 |
| **GO-LU-T** | 131.25 | 3132 | 63 | 12.05 | 22 | 4.21 | 41 | 7.84 | 523 |
| **GO-LU-22** | 131 | 1845 | 157 | 16.19 | 95 | 9.79 | 62 | 6.39 | 970 |
| **GO-LU-126** | 130.75 | 1642 | 100 | 18.73 | 65 | 12.17 | 35 | 6.55 | 534 |
| **GO-LU-S** | 130.25 | 1702 | 94 | 19.03 | 65 | 13.16 | 29 | 5.87 | 494 |
| **GO-LU-125** | 130 | 4162 | 45 | 8.43 | 20 | 3.75 | 25 | 4.68 | 534 |
| **GO-LU-21** | 129.75 | 3022 | 105 | 10.13 | 47 | 4.53 | 58 | 5.59 | 1037 |
| **GO-LU-R** | 129.25 | 1574 | 134 | 24.36 | 92 | 16.73 | 42 | 7.64 | 550 |
| **GO-LU-124** | 129 | 1872 | 149 | 26.47 | 107 | 18.98 | 42 | 7.49 | 561 |

| SAMPLE | Stratigraphic position (m) | Autochthonous specimens per mm$^2$ | REWORKED SPECIMENS | | MESOZOIC REWORKED | | CENOZOIC REWORKED | | Total counted specimens in first round |
|---|---|---|---|---|---|---|---|---|---|
| | | | Raw value | Percentage per total amount of specimens | Raw value | % total specimens | Raw value | % total specimens | |
| **GO-LU-20** | 128.75 | 1840 | 181 | 19.31 | 116 | 12.37 | 65 | 6.93 | 938 |
| **GO-LU-123** | 128.5 | 2006 | 118 | 23.55 | 64 | 12.77 | 54 | 10.78 | 501 |
| **GO-LU-Q** | 128.25 | 1625 | 120 | 25.10 | 84 | 17.57 | 36 | 7.53 | 478 |
| **GO-LU-19** | 127.75 | 3312 | 122 | 11.10 | 53 | 4.80 | 69 | 6.30 | 1095 |
| **GO-LU-P** | 127.4 | 1766 | 122 | 23.87 | 75 | 14.68 | 47 | 9.20 | 511 |
| **GO-LU-18** | 127.2 | 2844 | 131 | 19.44 | 64 | 9.50 | 67 | 9.94 | 674 |
| **GO-LU-122** | 127 | 1820 | 155 | 27.88 | 97 | 17.45 | 58 | 10.43 | 556 |
| **GO-LU-17** | 126.5 | 1674 | 161 | 17.44 | 77 | 8.34 | 84 | 9.10 | 923 |
| **GO-LU-Δ** | 126 | 2816 | 76 | 14.31 | 30 | 5.65 | 46 | 8.66 | 531 |
| **GO-LU-16** | 125.85 | 1529 | 183 | 16.92 | 110 | 10.17 | 73 | 6.75 | 1082 |
| **GO-LU-O** | 125.7 | 1036 | 163 | 31.77 | 115 | 22.42 | 48 | 9.36 | 513 |
| **GO-LU-121** | 125.5 | 6031 | 53 | 9.07 | 21 | 3.59 | 32 | 5.47 | 585 |
| **GO-LU-γ** | 125.3 | 2204 | 168 | 32.06 | 113 | 21.56 | 55 | 10.50 | 524 |
| **GO-LU-Ñ** | 125 | 1859 | 143 | 28.71 | 100 | 20.08 | 43 | 8.63 | 498 |
| **GO-LU-120** | 124.85 | 1972 | 112 | 21.64 | 86 | 16.62 | 26 | 5.02 | 518 |
| **GO-LU-15** | 124.7 | 2210 | 108 | 20.38 | 67 | 12.64 | 41 | 7.74 | 530 |
| **GO-LU-14** | 124.1 | 2234 | 170 | 13.90 | 79 | 6.44 | 91 | 7.46 | 1220 |
| **GO-LU-119** | 123.9 | 1589 | 173 | 33.08 | 123 | 23.52 | 50 | 9.56 | 523 |
| **GO-LU-N** | 123.75 | 1843 | 144 | 27.53 | 104 | 19.89 | 40 | 7.65 | 523 |
| **GO-LU-118** | 123.4 | 1123 | 172 | 34.26 | 145 | 28.88 | 27 | 5.38 | 502 |
| **GO-LU-13** | 122.7 | 2281 | 137 | 25.42 | 98 | 18.18 | 39 | 7.24 | 539 |
| **GO-LU-M** | 122.5 | 1419 | 156 | 28.26 | 114 | 20.65 | 42 | 7.61 | 552 |
| **GO-LU-117** | 122.3 | 4776 | 66 | 11.85 | 31 | 5.57 | 35 | 6.28 | 557 |
| **GO-LU-L** | 122.1 | 1083 | 123 | 26.00 | 93 | 19.66 | 30 | 6.34 | 473 |
| **GO-LU-12** | 121.85 | 1144 | 181 | 18.02 | 101 | 10.05 | 80 | 7.96 | 1005 |
| **GO-LU-116** | 121.6 | 809 | 207 | 40.12 | 150 | 29.07 | 57 | 11.05 | 516 |
| **GO-LU-K** | 121.25 | 1125 | 168 | 32.62 | 118 | 22.91 | 50 | 9.71 | 515 |
| **GO-LU-11** | 121 | 1305 | 205 | 18.19 | 110 | 9.78 | 95 | 8.40 | 1125 |
| **GO-LU-10** | 119 | 1869 | 223 | 19.75 | 137 | 12.13 | 86 | 7.62 | 1129 |
| **GO-LU-J** | 118.85 | 869 | 126 | 28.31 | 84 | 18.88 | 42 | 9.44 | 445 |
| **GO-LU-115** | 118.75 | 794 | 183 | 36.75 | 143 | 28.71 | 40 | 8.03 | 498 |
| **GO-LU-β** | 118.65 | 2257 | 100 | 18.83 | 54 | 10.17 | 46 | 8.66 | 531 |
| **GO-LU-09** | 118.5 | 1469 | 173 | 22.27 | 100 | 12.87 | 73 | 9.40 | 777 |
| **GO-LU-114** | 118.35 | 1377 | 174 | 32.34 | 103 | 19.14 | 71 | 13.20 | 538 |
| **GO-LU-α** | 118.2 | 2047 | 46 | 9.26 | 16 | 3.22 | 30 | 6.04 | 497 |
| **GO-LU-I** | 118 | 1834 | 71 | 14.95 | 33 | 6.95 | 38 | 8.00 | 475 |
| **GO-LU-08** | 117.75 | 3336 | 191 | 16.31 | 116 | 9.91 | 75 | 6.40 | 1171 |
| **GO-LU-113** | 117.5 | 5019 | 65 | 11.19 | 28 | 4.82 | 37 | 6.37 | 581 |
| **GO-LU-112b** | 117 | 4204 | 73 | 12.87 | 39 | 6.88 | 34 | 6.00 | 567 |
| **GO-LU-112a** | 116.6 | 6754 | 35 | 6.59 | 14 | 2.64 | 21 | 3.95 | 531 |
| **GO-LU-07** | 116.45 | 4655 | 55 | 9.14 | 20 | 3.32 | 35 | 5.81 | 602 |
| **GO-LU-H** | 116.3 | 2928 | 96 | 18.25 | 64 | 12.17 | 32 | 6.08 | 526 |
| **GO-LU-111c** | 116.15 | 5935 | 55 | 9.52 | 30 | 5.19 | 25 | 4.33 | 578 |
| **GO-LU-06** | 116 | 2743 | 101 | 8.75 | 45 | 3.88 | 56 | 4.88 | 1148 |
| **GO-LU-G** | 115.75 | 2463 | 43 | 9.01 | 12 | 2.52 | 31 | 6.50 | 477 |
| **GO-LU-05** | 115.5 | 2436 | 163 | 13.18 | 84 | 6.79 | 79 | 6.39 | 1237 |
| **GO-LU-111b** | 115.25 | 2519 | 125 | 25.25 | 71 | 14.34 | 54 | 10.91 | 495 |
| **GO-LU-111a** | 115 | 1719 | 65 | 12.51 | 28 | 5.39 | 37 | 7.12 | 520 |
| **GO-LU-F** | 114.75 | 2315 | 84 | 15.97 | 39 | 7.41 | 45 | 8.56 | 526 |
| **GO-LU-04** | 113.5 | 3449 | 166 | 11.19 | 64 | 4.32 | 102 | 6.88 | 1483 |
| **GO-LU-110** | 113.25 | 4542 | 55 | 10.54 | 18 | 3.45 | 37 | 7.09 | 522 |
| **GO-LU-03** | 112.5 | 3738 | 131 | 10.17 | 45 | 3.47 | 86 | 6.70 | 1284 |
| **GO-LU-E** | 112 | 4026 | 75 | 13.69 | 33 | 6.02 | 42 | 7.66 | 548 |
| **GO-LU-109** | 111.5 | 4572 | 86 | 15.47 | 21 | 3.78 | 65 | 11.69 | 556 |
| **GO-LU-D** | 111 | 2417 | 82 | 16.14 | 44 | 8.66 | 38 | 7.48 | 508 |
| **GO-LU-108** | 109.9 | 3987 | 105 | 18.31 | 64 | 11.16 | 41 | 7.15 | 574 |
| **GO-LU-107** | 108.5 | 1870 | 128 | 23.70 | 76 | 14.07 | 52 | 9.63 | 540 |
| **GO-LU-C** | 108 | 2363 | 121 | 25.85 | 76 | 16.24 | 45 | 9.62 | 468 |
| **GO-LU-01** | 107.5 | 3450 | 106 | 14.85 | 37 | 5.18 | 69 | 9.66 | 714 |
| **GO-LU-106X** | 106.75 | 2215 | 89 | 17.38 | 57 | 11.13 | 32 | 6.25 | 512 |
| **GO-LU-106** | 106.25 | 2807 | 136 | 26.82 | 87 | 17.16 | 49 | 9.66 | 507 |
| **GO-LU-105** | 105.5 | 2003 | 166 | 31.98 | 113 | 21.77 | 53 | 10.21 | 519 |
| **GO-LU-104** | 104.9 | 1547 | 122 | 22.98 | 76 | 14.31 | 46 | 8.66 | 531 |
| **GO-LU-B** | 104.25 | 2273 | 100 | 18.73 | 59 | 11.05 | 41 | 7.68 | 534 |
| **GO-LU-00** | 103.75 | 2985 | 117 | 10.78 | 42 | 3.84 | 75 | 6.94 | 1081 |
| **GO-LU-103** | 102.35 | 5458 | 57 | 10.59 | 28 | 5.20 | 29 | 5.39 | 538 |
| **GO-LU-102** | 101.75 | 1802 | 119 | 23.06 | 72 | 13.95 | 47 | 9.11 | 516 |
| **GO-LU-101** | 100.5 | 1467 | 99 | 16.65 | 59 | 9.92 | 40 | 6.73 | 595 |
| **GO-LU-A** | 99.25 | 1834 | 105 | 21.78 | 54 | 11.20 | 51 | 10.58 | 482 |
| **GO-LU-100** | 98 | 2082 | 75 | 14.91 | 36 | 7.16 | 39 | 7.75 | 503 |

| SAMPLE | Stratigraphic position (m) | Raw value of *Zygrhablithus bijugatus* per mm² | Warm and oligotrophic taxa | | "Near shore" taxa | | Total counted specimens in first round |
|---|---|---|---|---|---|---|---|
| | | | Raw value | Percentage per total amount of autochthonous specimens | Raw value | % autochthonous | |
| **GO-LU-156** | 179.2 | 68 | 47 | 10.22 | 19 | 4.13 | 514 |
| **GO-LU-155** | 177.9 | 68 | 46 | 9.96 | 10 | 2.60 | 531 |
| **GO-LU-154** | 174.5 | 62 | 34 | 7.84 | 12 | 2.65 | 522 |
| **GO-LU-153** | 173 | 170 | 54 | 10.95 | 12 | 2.43 | 547 |
| **GO-LU-152** | 169.8 | 148 | 52 | 11.40 | 6 | 1.75 | 525 |
| **GO-LU-151** | 167.8 | 88 | 50 | 11.39 | 13 | 3.19 | 535 |
| **GO-LU-150** | 166.9 | 136 | 62 | 12.26 | 5 | 1.00 | 552 |
| **GO-LU-149** | 165.75 | 91 | 48 | 9.96 | 13 | 2.90 | 521 |
| **GO-LU-148** | 164.5 | 119 | 58 | 12.26 | 8 | 1.69 | 534 |
| **GO-LU-147** | 162.5 | 63 | 51 | 10.25 | 4 | 0.70 | 544 |
| **GO-LU-146b** | 160.5 | 54 | 36 | 7.96 | 16 | 3.76 | 495 |
| **GO-LU-146a** | 159.75 | 73 | 46 | 9.39 | 12 | 2.45 | 530 |
| **GO-LU-145** | 158 | 105 | 65 | 13.49 | 5 | 1.26 | 517 |
| **GO-LU-144b** | 157.5 | 298 | 122 | 23.74 | 16 | 3.11 | 552 |
| **GO-LU-144a** | 156.7 | 83 | 66 | 13.52 | 8 | 1.84 | 538 |
| **GO-LU-143b** | 155.65 | 224 | 69 | 14.12 | 13 | 2.56 | 525 |
| **GO-LU-143a** | 154.9 | 102 | 58 | 11.32 | 9 | 1.76 | 552 |
| **GO-LU-142b** | 153.75 | 148 | 55 | 12.42 | 15 | 3.39 | 496 |
| **GO-LU-142a** | 153 | 106 | 50 | 11.67 | 12 | 2.71 | 535 |
| **GO-LU-141** | 152.25 | 179 | 46 | 9.51 | 8 | 1.86 | 561 |
| **GO-LU-140b** | 150.75 | 119 | 72 | 13.19 | 15 | 2.75 | 600 |
| **GO-LU-140a** | 150.25 | 170 | 48 | 10.54 | 8 | 1.98 | 518 |
| **GO-LU-139** | 149.6 | 31 | 33 | 6.94 | 6 | 1.16 | 544 |
| **GO-LU-138** | 148.75 | 116 | 42 | 9.93 | 9 | 2.84 | 526 |
| **GO-LU-137b** | 147.75 | 80 | 40 | 10.09 | 19 | 4.92 | 544 |
| **GO-LU-137a** | 147.25 | 86 | 49 | 10.95 | 16 | 3.58 | 578 |
| **GO-LU-30** | 146.75 | 340 | 174 | 16.20 | 29 | 2.65 | 1209 |
| **GO-LU-136** | 145.75 | 165 | 53 | 13.44 | 6 | 1.54 | 529 |
| **GO-LU-29** | 144.75 | 251 | 144 | 13.20 | 22 | 1.97 | 1212 |
| **GO-LU-135** | 144.5 | 51 | 38 | 10.84 | 5 | 1.45 | 524 |
| **GO-LU-28** | 143.5 | 143 | 55 | 11.96 | 11 | 2.39 | 556 |
| **GO-LU-134** | 143.25 | 91 | 38 | 10.27 | 4 | 1.10 | 466 |
| **GO-LU-Z** | 142.75 | 96 | 61 | 15.80 | 7 | 2.07 | 503 |
| **GO-LU-27** | 141.25 | 38 | 57 | 7.85 | 12 | 1.72 | 920 |
| **GO-LU-Y** | 140.75 | 24 | 46 | 10.60 | 4 | 0.92 | 533 |
| **GO-LU-133** | 140.5 | 156 | 31 | 6.11 | 8 | 1.58 | 553 |
| **GO-LU-132** | 139.5 | 115 | 56 | 15.49 | 13 | 3.46 | 526 |
| **GO-LU-131** | 138 | 165 | 57 | 13.32 | 11 | 2.57 | 515 |
| **GO-LU-26** | 137.5 | 521 | 224 | 22.30 | 46 | 4.53 | 1103 |
| **GO-LU-130** | 136.75 | 17 | 36 | 8.72 | 6 | 1.69 | 512 |
| **GO-LU-25** | 135.75 | 188 | 100 | 13.79 | 37 | 5.13 | 877 |
| **GO-LU-X** | 135.5 | 182 | 61 | 14.66 | 15 | 3.61 | 496 |
| **GO-LU-129** | 134.5 | 77 | 45 | 10.14 | 11 | 2.48 | 509 |
| **GO-LU-24** | 132.75 | 395 | 87 | 14.57 | 13 | 2.18 | 638 |
| **GO-LU-128** | 132.5 | 187 | 44 | 10.97 | 19 | 4.99 | 487 |
| **GO-LU-V** | 132.25 | 292 | 59 | 13.59 | 13 | 3.00 | 516 |
| **GO-LU-23** | 132 | 243 | 97 | 10.31 | 16 | 1.81 | 1042 |
| **GO-LU-127** | 131.75 | 494 | 96 | 18.90 | 24 | 4.72 | 553 |
| **GO-LU-U** | 131.5 | 204 | 59 | 14.86 | 12 | 3.53 | 502 |
| **GO-LU-T** | 131.25 | 313 | 89 | 19.35 | 18 | 3.91 | 523 |
| **GO-LU-22** | 131 | 89 | 97 | 11.87 | 25 | 3.14 | 970 |
| **GO-LU-126** | 130.75 | 106 | 47 | 10.83 | 15 | 3.46 | 534 |
| **GO-LU-S** | 130.25 | 132 | 61 | 15.25 | 12 | 3.00 | 494 |
| **GO-LU-125** | 130 | 255 | 48 | 9.82 | 16 | 3.27 | 534 |
| **GO-LU-21** | 129.75 | 201 | 112 | 11.96 | 35 | 3.76 | 1037 |
| **GO-LU-R** | 129.25 | 79 | 60 | 14.42 | 15 | 3.85 | 550 |
| **GO-LU-124** | 129 | 82 | 42 | 10.06 | 19 | 4.61 | 561 |
| **GO-LU-20** | 128.75 | 56 | 70 | 9.25 | 30 | 3.97 | 938 |
| **GO-LU-123** | 128.5 | 47 | 32 | 8.36 | 11 | 3.13 | 501 |
| **GO-LU-Q** | 128.25 | 109 | 34 | 9.50 | 7 | 1.96 | 478 |
| **GO-LU-19** | 127.75 | 180 | 106 | 10.84 | 19 | 2.00 | 1095 |
| **GO-LU-P** | 127.4 | 95 | 49 | 12.60 | 11 | 2.83 | 511 |
| **GO-LU-18** | 127.2 | 168 | 73 | 13.44 | 23 | 4.42 | 674 |
| **GO-LU-122** | 127 | 123 | 62 | 15.46 | 10 | 2.74 | 556 |
| **GO-LU-17** | 126.5 | 53 | 61 | 8.01 | 44 | 5.97 | 923 |
| **GO-LU-Δ** | 126 | 192 | 69 | 15.16 | 10 | 2.20 | 531 |
| **GO-LU-16** | 125.85 | 61 | 80 | 8.90 | 70 | 8.07 | 1082 |
| **GO-LU-O** | 125.7 | 27 | 21 | 6.00 | 22 | 6.29 | 513 |
| **GO-LU-121** | 125.5 | 522 | 73 | 13.73 | 41 | 7.62 | 585 |

| SAMPLE | Stratigraphic position (m) | Raw value of *Zygrhablithus bijugatus* per mm$^2$ | Warm and oligotrophic taxa | | "Near shore" taxa | | Total counted specimens in first round |
|---|---|---|---|---|---|---|---|
| | | | Raw value | Percentage per total amount of autochthonous specimens | Raw value | % autochthonous | |
| **GO-LU-γ** | 125.3 | 74 | 43 | 12.08 | 33 | 9.27 | 524 |
| **GO-LU-Ñ** | 125 | 79 | 46 | 12.96 | 22 | 6.20 | 498 |
| **GO-LU-120** | 124.85 | 131 | 62 | 15.29 | 11 | 2.96 | 518 |
| **GO-LU-15** | 124.7 | 120 | 38 | 9.00 | 14 | 3.32 | 530 |
| **GO-LU-14** | 124.1 | 83 | 104 | 9.86 | 27 | 2.52 | 1220 |
| **GO-LU-119** | 123.9 | 18 | 23 | 6.57 | 7 | 2.00 | 523 |
| **GO-LU-N** | 123.75 | 49 | 36 | 9.50 | 10 | 2.90 | 523 |
| **GO-LU-118** | 123.4 | 54 | 32 | 9.70 | 11 | 3.64 | 502 |
| **GO-LU-13** | 122.7 | 68 | 34 | 8.46 | 15 | 3.73 | 539 |
| **GO-LU-M** | 122.5 | 54 | 39 | 9.85 | 11 | 3.03 | 552 |
| **GO-LU-117** | 122.3 | 58 | 40 | 8.15 | 8 | 1.63 | 557 |
| **GO-LU-L** | 122.1 | 28 | 31 | 8.86 | 5 | 1.43 | 473 |
| **GO-LU-12** | 121.85 | 13 | 48 | 5.77 | 32 | 3.89 | 1005 |
| **GO-LU-116** | 121.6 | 45 | 41 | 13.27 | 12 | 4.21 | 516 |
| **GO-LU-K** | 121.25 | 71 | 52 | 14.99 | 11 | 3.17 | 515 |
| **GO-LU-11** | 121 | 37 | 74 | 7.99 | 30 | 3.37 | 1125 |
| **GO-LU-10** | 119 | 58 | 114 | 12.58 | 61 | 6.68 | 1129 |
| **GO-LU-J** | 118.85 | 27 | 37 | 11.60 | 26 | 8.15 | 445 |
| **GO-LU-115** | 118.75 | 45 | 52 | 16.51 | 30 | 9.37 | 498 |
| **GO-LU-β** | 118.65 | 21 | 37 | 8.58 | 5 | 1.62 | 531 |
| **GO-LU-09** | 118.5 | 68 | 53 | 8.69 | 51 | 8.44 | 777 |
| **GO-LU-114** | 118.35 | 64 | 50 | 13.74 | 25 | 6.87 | 538 |
| **GO-LU-α** | 118.2 | 123 | 81 | 17.96 | 16 | 3.55 | 497 |
| **GO-LU-I** | 118 | 5 | 39 | 9.65 | 6 | 1.49 | 475 |
| **GO-LU-08** | 117.75 | 126 | 100 | 10.15 | 22 | 2.19 | 1171 |
| **GO-LU-113** | 117.5 | 195 | 66 | 12.79 | 7 | 1.36 | 581 |
| **GO-LU-112b** | 117 | 196 | 48 | 9.72 | 16 | 3.24 | 567 |
| **GO-LU-112a** | 116.6 | 204 | 51 | 10.28 | 15 | 3.02 | 531 |
| **GO-LU-07** | 116.45 | 204 | 56 | 10.24 | 5 | 0.91 | 602 |
| **GO-LU-H** | 116.3 | 89 | 39 | 9.07 | 6 | 1.40 | 526 |
| **GO-LU-111c** | 116.15 | 533 | 83 | 15.87 | 20 | 3.82 | 578 |
| **GO-LU-06** | 116 | 139 | 169 | 16.09 | 47 | 4.49 | 1148 |
| **GO-LU-G** | 115.75 | 170 | 90 | 20.74 | 27 | 6.22 | 477 |
| **GO-LU-05** | 115.5 | 186 | 172 | 15.98 | 63 | 6.57 | 1237 |
| **GO-LU-111b** | 115.25 | 143 | 51 | 13.78 | 19 | 5.68 | 495 |
| **GO-LU-111a** | 115 | 57 | 52 | 11.44 | 13 | 2.97 | 520 |
| **GO-LU-F** | 114.75 | 110 | 67 | 15.16 | 17 | 4.07 | 526 |
| **GO-LU-04** | 113.5 | 141 | 162 | 12.30 | 54 | 4.29 | 1483 |
| **GO-LU-110** | 113.25 | 379 | 77 | 16.49 | 11 | 2.78 | 522 |
| **GO-LU-03** | 112.5 | 263 | 208 | 18.04 | 49 | 4.47 | 1284 |
| **GO-LU-E** | 112 | 170 | 60 | 12.68 | 16 | 4.44 | 548 |
| **GO-LU-109** | 111.5 | 97 | 42 | 8.94 | 12 | 2.55 | 556 |
| **GO-LU-D** | 111 | 176 | 68 | 15.96 | 16 | 4.69 | 508 |
| **GO-LU-108** | 109.9 | 196 | 50 | 10.57 | 16 | 3.42 | 574 |
| **GO-LU-107** | 108.5 | 104 | 66 | 16.02 | 7 | 1.94 | 540 |
| **GO-LU-C** | 108 | 157 | 58 | 16.71 | 3 | 0.86 | 468 |
| **GO-LU-01** | 107.5 | 227 | 108 | 17.76 | 13 | 2.30 | 714 |
| **GO-LU-106X** | 106.75 | 178 | 60 | 14.18 | 13 | 3.31 | 512 |
| **GO-LU-106** | 106.25 | 121 | 46 | 12.40 | 7 | 2.43 | 507 |
| **GO-LU-105** | 105.5 | 62 | 39 | 11.05 | 6 | 1.98 | 519 |
| **GO-LU-104** | 104.9 | 53 | 44 | 10.76 | 16 | 4.16 | 531 |
| **GO-LU-B** | 104.25 | 141 | 62 | 14.29 | 8 | 2.07 | 534 |
| **GO-LU-00** | 103.75 | 427 | 224 | 23.22 | 57 | 5.96 | 1081 |
| **GO-LU-103** | 102.35 | 363 | 60 | 12.47 | 15 | 3.33 | 538 |
| **GO-LU-102** | 101.75 | 100 | 43 | 10.83 | 27 | 7.30 | 516 |
| **GO-LU-101** | 100.5 | 83 | 65 | 13.02 | 12 | 2.62 | 595 |
| **GO-LU-A** | 99.25 | 63 | 56 | 14.85 | 10 | 2.65 | 482 |
| **GO-LU-100** | 98 | 68 | 41 | 9.58 | 12 | 2.80 | 503 |

| SAMPLE | Stratigraphic position (m) | *Reticulofenestra minuta* | | *Reticulofenestra dictyoda* | | *Coccolithus* spp | | Total counted specimens in first round |
|---|---|---|---|---|---|---|---|---|
| | | Raw value | % autochthonous | Raw value | % autochthonous | Raw value | % autochthonous | |
| **GO-LU-156** | 179.2 | 200 | 43.48 | 86 | 18.70 | 74 | 16.09 | 514 |
| **GO-LU-155** | 177.9 | 184 | 39.83 | 114 | 24.68 | 70 | 15.15 | 531 |
| **GO-LU-154** | 174.5 | 155 | 35.76 | 125 | 28.84 | 75 | 17.30 | 522 |
| **GO-LU-153** | 173 | 210 | 42.60 | 122 | 24.75 | 70 | 14.10 | 547 |
| **GO-LU-152** | 169.8 | 153 | 33.55 | 138 | 30.26 | 69 | 15.13 | 525 |
| **GO-LU-151** | 167.8 | 163 | 37.13 | 113 | 25.74 | 67 | 15.26 | 535 |
| **GO-LU-150** | 166.9 | 156 | 31.11 | 181 | 36.09 | 70 | 13.96 | 552 |
| **GO-LU-149** | 165.75 | 167 | 34.65 | 169 | 35.06 | 51 | 10.58 | 521 |
| **GO-LU-148** | 164.5 | 140 | 29.60 | 150 | 31.71 | 81 | 17.12 | 534 |
| **GO-LU-147** | 162.5 | 156 | 31.36 | 184 | 36.98 | 78 | 15.68 | 544 |
| **GO-LU-146b** | 160.5 | 132 | 29.20 | 157 | 34.73 | 77 | 17.04 | 495 |
| **GO-LU-146a** | 159.75 | 177 | 36.12 | 138 | 28.16 | 87 | 17.76 | 530 |
| **GO-LU-145** | 158 | 164 | 34.31 | 136 | 28.45 | 84 | 17.57 | 517 |
| **GO-LU-144b** | 157.5 | 142 | 27.63 | 126 | 24.51 | 86 | 16.73 | 552 |
| **GO-LU-144a** | 156.7 | 161 | 32.99 | 136 | 27.87 | 80 | 16.39 | 538 |
| **GO-LU-143b** | 155.65 | 148 | 30.30 | 165 | 33.78 | 63 | 12.90 | 525 |
| **GO-LU-143a** | 154.9 | 176 | 34.34 | 157 | 30.63 | 87 | 16.98 | 552 |
| **GO-LU-142b** | 153.75 | 155 | 34.99 | 116 | 26.19 | 77 | 17.38 | 496 |
| **GO-LU-142a** | 153 | 159 | 37.50 | 80 | 18.87 | 86 | 20.28 | 535 |
| **GO-LU-141** | 152.25 | 187 | 38.68 | 123 | 25.44 | 92 | 18.92 | 561 |
| **GO-LU-140b** | 150.75 | 185 | 33.88 | 126 | 23.08 | 109 | 19.96 | 600 |
| **GO-LU-140a** | 150.25 | 170 | 37.32 | 133 | 29.20 | 67 | 14.71 | 518 |
| **GO-LU-139** | 149.6 | 191 | 40.17 | 123 | 25.87 | 88 | 18.51 | 544 |
| **GO-LU-138** | 148.75 | 172 | 40.66 | 88 | 20.80 | 71 | 16.78 | 526 |
| **GO-LU-137b** | 147.75 | 123 | 31.02 | 94 | 23.71 | 81 | 20.43 | 544 |
| **GO-LU-137a** | 147.25 | 168 | 37.54 | 77 | 17.21 | 89 | 19.89 | 578 |
| **GO-LU-30** | 146.75 | 454 | 42.27 | 229 | 21.32 | 98 | 9.12 | 1209 |
| **GO-LU-136** | 145.75 | 139 | 35.60 | 76 | 19.46 | 73 | 18.69 | 529 |
| **GO-LU-29** | 144.75 | 420 | 38.50 | 259 | 23.74 | 143 | 13.11 | 1212 |
| **GO-LU-135** | 144.5 | 83 | 23.99 | 101 | 29.19 | 78 | 22.54 | 524 |
| **GO-LU-28** | 143.5 | 165 | 35.87 | 114 | 24.78 | 62 | 13.48 | 556 |
| **GO-LU-134** | 143.25 | 134 | 36.71 | 81 | 22.19 | 80 | 21.92 | 466 |
| **GO-LU-Z** | 142.75 | 114 | 29.53 | 104 | 26.94 | 58 | 15.03 | 503 |
| **GO-LU-27** | 141.25 | 260 | 35.79 | 177 | 24.36 | 119 | 16.38 | 920 |
| **GO-LU-Y** | 140.75 | 112 | 25.81 | 159 | 36.64 | 80 | 18.43 | 533 |
| **GO-LU-133** | 140.5 | 159 | 31.36 | 190 | 37.48 | 96 | 18.93 | 553 |
| **GO-LU-132** | 139.5 | 87 | 24.07 | 64 | 17.70 | 92 | 25.45 | 526 |
| **GO-LU-131** | 138 | 169 | 39.49 | 75 | 17.52 | 74 | 17.29 | 515 |
| **GO-LU-26** | 137.5 | 349 | 34.74 | 202 | 20.11 | 104 | 10.35 | 1103 |
| **GO-LU-130** | 136.75 | 135 | 32.69 | 103 | 24.94 | 90 | 21.79 | 512 |
| **GO-LU-25** | 135.75 | 219 | 30.35 | 182 | 25.23 | 110 | 15.25 | 877 |
| **GO-LU-X** | 135.5 | 133 | 31.97 | 107 | 25.72 | 64 | 15.38 | 496 |
| **GO-LU-129** | 134.5 | 199 | 44.82 | 100 | 22.52 | 50 | 11.26 | 509 |
| **GO-LU-24** | 132.75 | 185 | 30.99 | 201 | 33.67 | 68 | 11.39 | 638 |
| **GO-LU-128** | 132.5 | 149 | 37.16 | 80 | 19.95 | 68 | 16.96 | 487 |
| **GO-LU-V** | 132.25 | 154 | 35.48 | 101 | 23.27 | 67 | 15.44 | 516 |
| **GO-LU-23** | 132 | 405 | 43.04 | 187 | 19.87 | 154 | 16.37 | 1042 |
| **GO-LU-127** | 131.75 | 136 | 26.77 | 103 | 20.28 | 97 | 19.09 | 553 |
| **GO-LU-U** | 131.5 | 96 | 24.18 | 103 | 25.94 | 85 | 21.41 | 502 |
| **GO-LU-T** | 131.25 | 143 | 31.09 | 96 | 20.87 | 77 | 16.74 | 523 |
| **GO-LU-22** | 131 | 339 | 41.70 | 159 | 19.56 | 105 | 12.92 | 970 |
| **GO-LU-126** | 130.75 | 155 | 35.71 | 93 | 21.43 | 84 | 19.35 | 534 |
| **GO-LU-S** | 130.25 | 105 | 26.25 | 102 | 25.50 | 82 | 20.50 | 494 |
| **GO-LU-125** | 130 | 162 | 33.13 | 149 | 30.47 | 67 | 13.70 | 534 |
| **GO-LU-21** | 129.75 | 367 | 39.38 | 231 | 24.79 | 113 | 12.12 | 1037 |
| **GO-LU-R** | 129.25 | 108 | 25.96 | 127 | 30.53 | 61 | 14.66 | 550 |
| **GO-LU-124** | 129 | 109 | 26.42 | 125 | 30.30 | 75 | 18.18 | 561 |
| **GO-LU-20** | 128.75 | 319 | 42.17 | 146 | 19.30 | 102 | 13.48 | 938 |
| **GO-LU-123** | 128.5 | 134 | 34.99 | 88 | 22.98 | 79 | 20.63 | 501 |
| **GO-LU-Q** | 128.25 | 106 | 29.61 | 119 | 33.24 | 59 | 16.48 | 478 |
| **GO-LU-19** | 127.75 | 372 | 38.23 | 271 | 27.85 | 118 | 12.13 | 1095 |
| **GO-LU-P** | 127.4 | 129 | 33.16 | 82 | 21.08 | 70 | 17.99 | 511 |
| **GO-LU-18** | 127.2 | 150 | 27.62 | 161 | 29.65 | 81 | 14.92 | 674 |
| **GO-LU-122** | 127 | 98 | 24.44 | 77 | 19.20 | 85 | 21.20 | 556 |
| **GO-LU-17** | 126.5 | 351 | 46.06 | 113 | 14.83 | 97 | 12.73 | 923 |
| **GO-LU-Δ** | 126 | 109 | 23.96 | 126 | 27.69 | 87 | 19.12 | 531 |
| **GO-LU-16** | 125.85 | 412 | 45.85 | 144 | 16.03 | 82 | 9.13 | 1082 |
| **GO-LU-O** | 125.7 | 121 | 34.57 | 60 | 17.14 | 64 | 18.29 | 513 |
| **GO-LU-121** | 125.5 | 207 | 38.95 | 105 | 19.76 | 75 | 14.11 | 585 |
| **GO-LU-γ** | 125.3 | 118 | 33.15 | 61 | 17.13 | 62 | 17.42 | 524 |
| **GO-LU-Ñ** | 125 | 121 | 34.08 | 63 | 17.75 | 57 | 16.06 | 498 |

| SAMPLE | Stratigraphic position (m) | *Reticulofenestra minuta* | | *Reticulofenestra dictyoda* | | *Coccolithus* spp | | Total counted specimens in first round |
|---|---|---|---|---|---|---|---|---|
| | | Raw value | % autochthonous | Raw value | % autochthonous | Raw value | % autochthonous | |
| **GO-LU-120** | 124.85 | 140 | 34.53 | 81 | 19.98 | 76 | 18.74 | 518 |
| **GO-LU-15** | 124.7 | 130 | 30.81 | 97 | 22.99 | 77 | 18.25 | 530 |
| **GO-LU-14** | 124.1 | 535 | 50.95 | 199 | 18.95 | 100 | 9.52 | 1220 |
| **GO-LU-119** | 123.9 | 91 | 26.00 | 112 | 32.00 | 80 | 22.86 | 523 |
| **GO-LU-N** | 123.75 | 129 | 34.04 | 91 | 24.01 | 60 | 15.83 | 523 |
| **GO-LU-118** | 123.4 | 96 | 29.09 | 87 | 26.36 | 61 | 18.48 | 502 |
| **GO-LU-13** | 122.7 | 176 | 43.78 | 89 | 22.14 | 47 | 11.69 | 539 |
| **GO-LU-M** | 122.5 | 162 | 40.91 | 78 | 19.70 | 60 | 15.15 | 552 |
| **GO-LU-117** | 122.3 | 166 | 33.81 | 164 | 33.40 | 77 | 15.68 | 557 |
| **GO-LU-L** | 122.1 | 104 | 29.71 | 125 | 35.71 | 52 | 14.86 | 473 |
| **GO-LU-12** | 121.85 | 353 | 42.87 | 215 | 26.11 | 92 | 11.17 | 1005 |
| **GO-LU-116** | 121.6 | 97 | 31.39 | 68 | 22.01 | 54 | 17.48 | 516 |
| **GO-LU-K** | 121.25 | 131 | 37.75 | 61 | 17.58 | 45 | 12.97 | 515 |
| **GO-LU-11** | 121 | 447 | 48.59 | 169 | 18.37 | 108 | 11.68 | 1125 |
| **GO-LU-10** | 119 | 303 | 33.44 | 199 | 21.96 | 103 | 11.37 | 1129 |
| **GO-LU-J** | 118.85 | 112 | 35.11 | 45 | 14.11 | 46 | 14.42 | 445 |
| **GO-LU-115** | 118.75 | 25 | 7.94 | 86 | 27.30 | 72 | 22.86 | 498 |
| **GO-LU-β** | 118.65 | 193 | 44.78 | 85 | 19.72 | 57 | 13.23 | 531 |
| **GO-LU-09** | 118.5 | 247 | 40.89 | 105 | 17.38 | 68 | 11.26 | 777 |
| **GO-LU-114** | 118.35 | 120 | 32.97 | 62 | 17.03 | 58 | 15.93 | 538 |
| **GO-LU-α** | 118.2 | 163 | 36.14 | 96 | 21.29 | 52 | 11.53 | 497 |
| **GO-LU-I** | 118 | 171 | 42.33 | 101 | 25.00 | 65 | 16.09 | 475 |
| **GO-LU-08** | 117.75 | 474 | 48.37 | 174 | 17.76 | 110 | 11.22 | 1171 |
| **GO-LU-113** | 117.5 | 179 | 34.69 | 142 | 27.52 | 79 | 15.31 | 581 |
| **GO-LU-112b** | 117 | 154 | 31.17 | 133 | 26.92 | 101 | 20.45 | 567 |
| **GO-LU-112a** | 116.6 | 118 | 23.79 | 180 | 36.29 | 89 | 17.94 | 531 |
| **GO-LU-07** | 116.45 | 153 | 27.97 | 207 | 37.84 | 68 | 12.43 | 602 |
| **GO-LU-H** | 116.3 | 202 | 46.98 | 64 | 14.88 | 86 | 20.00 | 526 |
| **GO-LU-111c** | 116.15 | 144 | 27.53 | 139 | 26.58 | 90 | 17.21 | 578 |
| **GO-LU-06** | 116 | 312 | 29.79 | 287 | 27.40 | 130 | 12.41 | 1148 |
| **GO-LU-G** | 115.75 | 156 | 35.94 | 68 | 15.67 | 72 | 16.59 | 477 |
| **GO-LU-05** | 115.5 | 338 | 31.49 | 222 | 20.68 | 133 | 12.39 | 1237 |
| **GO-LU-111b** | 115.25 | 116 | 31.35 | 74 | 20.00 | 49 | 13.24 | 495 |
| **GO-LU-111a** | 115 | 220 | 48.40 | 64 | 14.08 | 57 | 12.54 | 520 |
| **GO-LU-F** | 114.75 | 158 | 35.75 | 110 | 24.89 | 62 | 14.03 | 526 |
| **GO-LU-04** | 113.5 | 597 | 45.33 | 202 | 15.34 | 162 | 12.30 | 1483 |
| **GO-LU-110** | 113.25 | 131 | 28.05 | 147 | 31.48 | 68 | 14.56 | 522 |
| **GO-LU-03** | 112.5 | 314 | 27.23 | 316 | 27.41 | 137 | 11.88 | 1284 |
| **GO-LU-E** | 112 | 138 | 29.18 | 135 | 28.54 | 74 | 15.64 | 548 |
| **GO-LU-109** | 111.5 | 159 | 33.83 | 144 | 30.64 | 64 | 13.62 | 556 |
| **GO-LU-D** | 111 | 103 | 24.18 | 122 | 28.64 | 73 | 17.14 | 508 |
| **GO-LU-108** | 109.9 | 155 | 33.08 | 140 | 29.88 | 55 | 11.63 | 574 |
| **GO-LU-107** | 108.5 | 128 | 31.07 | 98 | 23.79 | 65 | 15.78 | 540 |
| **GO-LU-C** | 108 | 112 | 32.28 | 73 | 21.04 | 50 | 14.41 | 468 |
| **GO-LU-01** | 107.5 | 167 | 27.47 | 166 | 27.30 | 70 | 11.51 | 714 |
| **GO-LU-106X** | 106.75 | 133 | 31.44 | 94 | 22.22 | 78 | 18.44 | 512 |
| **GO-LU-106** | 106.25 | 118 | 31.81 | 100 | 26.95 | 62 | 16.71 | 507 |
| **GO-LU-105** | 105.5 | 97 | 27.48 | 106 | 30.03 | 58 | 16.43 | 519 |
| **GO-LU-104** | 104.9 | 139 | 33.99 | 96 | 23.47 | 57 | 13.94 | 531 |
| **GO-LU-B** | 104.25 | 140 | 32.26 | 98 | 22.58 | 64 | 14.75 | 534 |
| **GO-LU-00** | 103.75 | 310 | 32.14 | 123 | 12.75 | 136 | 14.10 | 1081 |
| **GO-LU-103** | 102.35 | 112 | 23.28 | 172 | 35.76 | 92 | 19.13 | 538 |
| **GO-LU-102** | 101.75 | 95 | 23.93 | 108 | 27.20 | 72 | 18.14 | 516 |
| **GO-LU-101** | 100.5 | 212 | 42.79 | 84 | 16.95 | 71 | 14.33 | 595 |
| **GO-LU-A** | 99.25 | 123 | 32.63 | 78 | 20.69 | 70 | 18.57 | 482 |
| **GO-LU-100** | 98 | 145 | 33.88 | 101 | 23.60 | 81 | 18.93 | 503 |